TECHNISCHE UNIVERSITÄT WIEN
Vienna University of Technology

DIPLOMARBEIT

IMPLICATIONS OF DIFFERENT SKY-MODELS FOR THE SIMULATION BASED PREDICTION OF INDOOR LIGHT LEVELS

ausgeführt zum Zwecke der Erlangung des

akademischen Grades eines Diplom-Ingenieurs

unter der Leitung von

Univ.Prof. Dipl.-Ing. Dr.techn. Ardeshir Mahdavi

E 259-3 Abteilung für Bauphysik und Bauökologie

Institut für Architekturwissenschaften

eingereicht an der

Technischen Universität Wien

Fakultät für Architektur und Raumplanung

von

Ghazal Etminan

Matrikelnr.1328704

Master Building Science and Technology

Wien, June 2016

KURZFASSUNG

Um den Einfall und die Verteilung von Tageslicht in architektonischen Räumen zu modellieren, benötigen Simulationsprogramme zuverlässige Definitionen von Randbedingungen in der Regel bezogen auf Verteilungsmodelle der Himmelsleuchtdichte.Die Auswirkungen der Fehler von Himmelsmodellen auf simulationsmodellbasierte Innenraumbeleuchtungsprognosen sind jedoch nicht ausreichend dokumentiert.

Es gibt verschiedene Werkzeuge und Methoden zur Simulation der Innenraumbeleuchtungsbedingungen und der damit verbundenen Tageslicht-Indikatoren. In der vorliegenden Studie, wurde das Lichtsimulationsprogramm Radiance gewählt. Um Himmelsszenenbeschreibungen zu generieren, enthält das Radiance-Simulationsprogramm zwei Routinen: Gendaylit und Gensky. Diese Routinen erfordern die Eingabe von Information über beide Komponenten der Solarstrahlung, der direkten und der diffusen Strahlung.

Um die Auswirkungen der Himmelsmodellauswahl auf die Plausibilität der Simulationsergebnisse zu untersuchen, wurde das Programm Radiance verwendet. die Innenraumbeleuchtungsstärke wurde in einem bestehenden Testraum auf dem Dach eines Universitätsgebäudes der TU Wien getestet. Dabei wurden die beiden zuvor genannten Himmelsmodelle berücksichtigt. Das dritte Modell Skyscanner (SC) ist ein Himmelsmodell, das auf Basis der mit einem Himmelscanner gemessenen Werte erzeugt erstellt wurde. Die Beleuchtungsstärken wurden in diesem Raum bei unterschiedlichen Außenbedingungen (klar, gering bewölkt, bedeckt) gemessen. Der Vergleich der Messungen mit den Ergebnissen mehreren mehrerer Modellsimulationen ermöglicht eine empirisch basierte Bewertung der Zuverlässigkeit von Innenraumbeleuchtungsprognosen, im Hinblick auf unterschiedliche Annahmen und entsprechend der herrschenden Rahmenbedingungen.

Schlüsselwörter

Beleuchtungsstärke, Himmelsmodell, Tageslicht, Sky scanner, Radiance

ABSTRACT

In order to model daylight availability and distribution in architectural spaces, simulation tools require reliable representations of boundary conditions – typically in terms of sky luminance distribution models. However, the impact of sky model errors on simulation-based indoor illuminance predictions is not well documented. There are different tools and methods to simulate indoor illuminance conditions and related daylight indicators.

In the present study, the Radiance lighting simulation program was selected. In order to generate sky scene description, Radiance contains two routines, Gendaylit and Gensky. These routines require, as input, information on both direct and diffuse components of solar radiation. To explore the implications of the sky model selection on the fidelity of simulation results, Radiance was used to compute the indoor illuminance in an existing test room on the rooftop of Technical University of Vienna. Therefore, the aforementioned two sky models were considered. A third option sky scanner (SC) was a sky model, generated via measured values obtained from a sky scanner. Simultaneously, the actual illuminance levels in the room were monitored under different outdoor conditions (clear, intermediate, and overcast).

A comparison of the measurement results, with the multiple model prediction results, facilitates an empirically based evaluation of the reliability of indoor illuminance predictions in the face of different assumptions pertaining to the prevailing boundary conditions.

Keywords

Illuminance, Sky models, Daylight, Sky scanner, Radiance

AKNOWLEDGMENTS

I would like to express my deepest gratitude to my supervisor, Professor Dr. Ardeshir Mahdavi, for his continuous support throughout this thesis and his patience with my endless questions. Furthermore, I would like to thank Mr Ehsan Vazifeh for selflessly sharing his knowledge with me. This masters thesis benefited from collaboration with Mr Vazifeh. Accordingly, the related material and text are in part incorporated in his PhD thesis “High-Resolution Sky Models for Building Performance Assessment“, which is funded by a grant from "Innovative Projekte”, TU Wien.

I would also like to thank members of the Department of Building Physics and Building Ecology, including Dr. Bob Martens, Dr. Matthias Schuss, and Mr. Josef Leichleitner for their support toward the completion of the thesis.

Last but not least, I would like to thank my amazing family and friends, to whom I owe everything, as without them none of this would even matter.

CONTENTS

1 INTRODUCTION

1.1 Overview

As energy performance and sustainability have become a crucial concern in modern architecture, daylighting is regarded as a vital tool in decreasing the energy consumption by minimizing the amount of electricity used for lighting in buildings during daytime (Kensek and Suk 2011). The latest improvements in computer systems have enabled architects to predict the luminance and interior daylighting of buildings. To support proper design of day-lit spaces, computational tools can be effectively deployed. Therefore, simulation can provide predictions of daylight distributions in spaces via virtual sensors (to measure illuminance, luminance, glare, etc.) positioned in building designs luminance, glare, etc. (Mahdavi 2008). As a result there has emerged a significant body of research on the subject of sky modeling to support reliable simulation-based estimation of indoor illuminance (Littlefair 1994). Such simulations require detailed sky luminance distribution models for the accurate prediction of daylight in indoor environments. However, the outcome of simulations is very sensitive to the assumptions related to sky luminance distribution.

In order to achieve the above, there is a need to create an accurate sky simulation model that produces a realistic prediction compared to real measurements. Progressively, more detailed sky luminance models have been developed for the prediction of daylight in buildings and for the implementation of simulation-based control systems (Dervishi 2010). Sky model evaluation is carried out by measuring the differences between modeled and measured sky luminance distribution (Littlefair 1994). However, there have been differences between the real sky luminance distribution and those predicted in models. The reason for these differences have not yet fully been explained or resolved; it has proved to be too difficult to discover the cause of these errors, which may lie in the basic algorithms or the representation of the sky condition in the models.

The objective of this thesis is to compare the performance of various sky models (CIE, Perez All Weather and Sky scanner) by predicting: i) the vertical irradiance on outside surfaces of a building, and ii) the horizontal and vertical illuminance levels on a room's interior surfaces. The results produced by these models were evaluated against measurements obtained from physical sensors to determine the performance of the sky models.

1.2 Motivation

Over the past decades, daylighting has emerged as a new potential source of energy saving for several reasons:

1. The European Commission encourages the integration of daylight utilization guidelines within building design rules, to reduce electrical energy consumption of artificial lighting (European Commission 2009).
2. Daylighting is an ideal lighting source that provides a much more desirable and pleasant interior environment for human living (Webb 2006). Numerous experts have examined the influence of daylight on:
    - Energy performance
    - Visual comfort
    - Human health
    - Work efficiency

Given the scarce resources available for future generations, increasing and volatile nature of energy prices and uncertainty of supply, efficient use of natural and freely available sources of energy such as natural daylighting has become vital in future building planning. In the next section we will explore the development of the tools for the effective prediction of natural delighting daylight in building design in the last century.

Incorporating sunlight into buildings boosts health and psychological behavior, in addition to sunlight being an endless source of energy (Chou 2004). Holick (2010) demonstrated that sun exposure generates Vitamin D, which is vital for regulating calcium in the body and bone formation. It is common knowledge that having windows in a workplace environment to achieve more daylighting is considered desirable, as most of us prefer natural light to artificial lighting in order to perform better at work. Occupants in offices would generally prefer to be positioned next to windows, where the daylight is stronger, to do their work (Leslie 2003). Proximity to windows is also believed to increase productivity, possibly due to the increase in work satisfaction and the decrease in fatigue that natural daylight brings.

At the same time, there is significant research relating to the negative effects of insufficient daylight. Baker and Steemers (2014) claim that using artificial light alone leads to anxiety, exhaustion and tension for people.

1.3 Background

1.3.1 Overview

For most of the 20th century, lighting requirements were mostly driven by our need to see. However, over the past 20 years or so this need has developed and evolved significantly to include not only vision but also a range of other needs, fields and definitions such as;

- *Architectural definition: the interplay of natural light and building form to provide a visually stimulating, healthful, and productive interior environment*
- *Lighting Energy Savings definition: the replacement of indoor electric illumination needs by daylight, resulting in reduced annual energy consumption for lighting*
- *Building Energy Consumption definition: the use of fenestration systems and responsive electric lighting controls to reduce overall building energy requirements (heating, cooling, lighting)*
- *Load Management definition: dynamic control of fenestration and lighting to manage and control building peak electric demand and load shape*
- *Cost definition: the use of daylighting strategies to minimize operating costs and maximize output, sales, or productivity* (Reinhart et al. 2006).

It is now universally known that natural light (as opposed to artificial lighting) positively affects human performance, as well as mental and physical health of people. According to Ott (1997), “the body uses light as a nutrient for metabolic processes similar to water or food. Natural light stimulates essential biological functions in the brain and is divided into colors that are vital to our health. On a cloudy day or under poor lighting conditions, the inability to perceive the colors from light can affect our mood and energy level”.

Robbins (1985) states that natural light is associated with higher energy levels, better mood and moral, and less stress on eyes. Another reason to use natural light is to meet the need for contact with nature.

Furthermore, the effects of direct sunlight and the resulting natural light have beneficial effects in two other ways: (i) through light reaching the retina affecting endocrine, hormone and metabolic state, and (ii) those resulting from sun on the skin such as the production of vitamin D (Edwards and Torcellini 2002).

From an economic point of view the benefits of natural lighting includes more productivity, reduced absenteeism, and other cost savings. Some countries in Europe require workers to be seated within 27 feet of a window (Robbins 1985). In buildings with a lack of daylighting, full-spectrum bright lights (commercially known as SAD – Seasonal Affective Disorder - lighting) are shown to positively affect people. According to Luo (1998) full-spectrum bright light allows day and night workers to adjust their internal clocks or circadian cycles. Studies show that the use of daylighting decreases the occurrence of headaches, SAD, and eyestrain (Franta and Anstead 1994).

Daylighting has emerged as a new potential source in energy saving. In order to gain accurate energy simulation, it is necessary to know daylighting conditions. Numerous sky luminance distribution models have been designed (Mahdavi 2008, 2001). The combination of an advanced simulation model and a detailed sky model that can appropriately match the local sky luminance distribution patterns is likely to provide reliable predictions of the daylight distribution in architectural spaces (Mahdavi 2005; Pal and Mahdavi 1999). For daylight simulation the Radiance program is used to construct sky luminance distribution patterns. The Radiance program has been validated rigorously. Different researchers (e.g. Mardaljevic 1999) have shown that this lighting simulation program achieves a high degree of accuracy. For the prediction of daylight supply in the room, the Radiance lighting simulation program needs illuminance as an input for sky model generation (Mahdavi and Dervishi 2010). Daylighting simulation, sky models and Radiance simulation engines are important aspects of these experiments that will be explored further below.

1.3.2 Daylighting Simulations

To support proper design of day-lit spaces, computational tools can be effectively deployed. Therefore, simulations can provide predictions of daylight distributions in spaces via virtual sensors (to measure illuminance, luminance, glare, etc.) positioned in building designs. Model-based building systems' control applications also use daylight simulation (Mahdavi et al. 1999). Daylighting simulation can estimate the amount of available daylight inside a building under one or several sky conditions. The principal goal of daylighting analysis is to provide a reliable prediction of a potential design to give the required level of natural illumination. The simulation output can be discrete numbers, such as luminance and illuminance, under selected sensor points with a scene or visualization of a scene. It is important to bear in mind that the quality and accuracy of simulation can be influenced by a number of different factors, such as; calculation methods, sky models, building models, surface properties and user expertise.

Simulation-based predictions cannot be expected to exactly match the conditions in real spaces, due to multiple uncertainties associated with the above data categories. Previous studies have suggested that simulation of daylight conditions can achieve a deviation of around 10% from actual measurements, and still be deemed acceptable (Mardaljevic 1995; Reinhart 2006; Reinhart and Andersen 2006; Reinhart and Walkenhorst 2001). Daylight simulation tools typically require a number of steps to compute indoor illuminance and luminance distribution. These include (Figure 1):

- Defining the building model (geometry, layout)
- Building properties (materials)
- Sky model (including sky conditions)
- Virtual sensors (viewpoint and grid of sensor points)

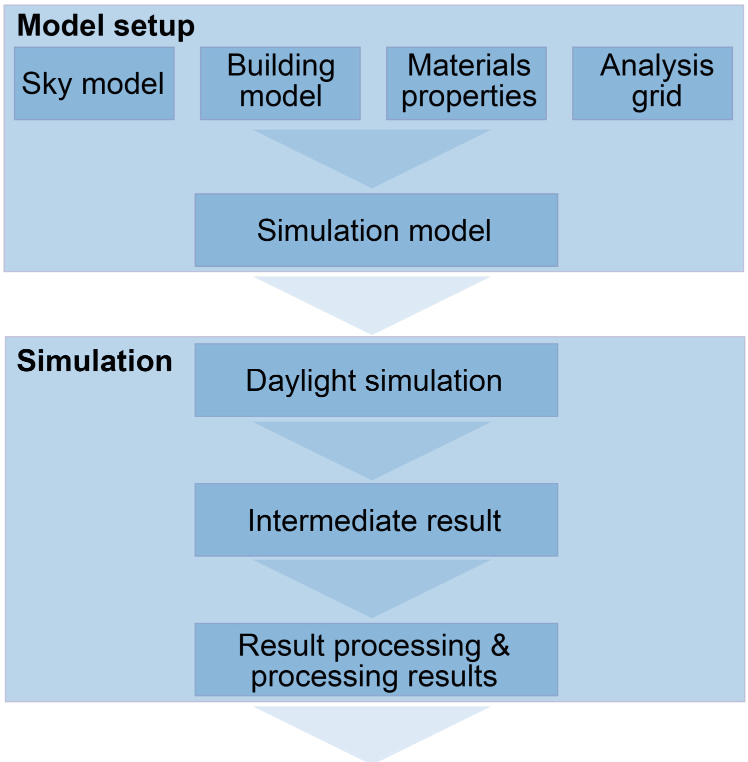

Figure 1 - Elements needed for a daylight simulation

Another requirement in daylighting simulation is choosing the daylighting simulation engine option, which are radiosity or ray tracing.

Surfaces are also an important area of consideration, as most people prefer natural daylight without glare. Therefore, from a design perspective a poor daylighting area will deliver either insufficient amounts of natural light, or high amounts of light but with a great deal of glare. In practice, however, illuminances in the range of 100 to 2500 lx are likely to result in significant reductions of artificial lighting usage in the home (National Association of Rooflight manufacture 2015).

All daylighting strategies make use of the luminance distribution from the sun, sky, buildings, and the ground. Daylight strategies depend on the availability of natural light, which is determined by the latitude of the building site and the conditions immediately surrounding the building, e.g. the presence of obstructions. Daylighting strategies are also affected by climate. Thus, the identification of seasonal prevailing climate conditions, particularly ambient temperatures and sunshine probability, is a basic step in daylight design. Studying both climate and daylight availability at a construction site is key to understanding the operating conditions of the building's facade. The daylighting design solution for the building should address all of these operating conditions (Ruck et al. 2000).

There are two methods of daylight simulations, static and dynamic methods, that differ depending on whether they consider a single or a series of consecutive sky conditions. In static daylight simulation we concentrate on the indoor illuminance distribution when the sky is overcast. The daylight factor is the most common parameter to characterize the daylight situation in buildings. On the other hand, a dynamic daylighting simulation method records the indoor illuminance under several sky conditions over a period of time. The concept of "daylight factor" was developed in the early 20th century in the United Kingdom (International Commission on Illumination 1970). It has the same basic definition as the sky factor, with the exception that daylight factor uses the CIE Standard overcast sky, instead of a uniform luminance sky. Daylight factor is more relevant for the prediction of daylight penetration to indoor space under overcast conditions, and less so in sunny conditions.

Daylight availability is similar to daylight factor, in that it is the ratio between indoor and outdoor illuminance levels. However, daylight availability is calculated under the actual sky conditions, which also includes clear and intermediate skies (Papa michael et al. 2013). Calculating daylight factor requires complex repetition of calculations and is generally undertaken using complex software such as Radiance. This is a suite of tools used for performing lighting simulation, which includes a renderer, as well as other tools for measuring and calculating simulated light levels, such as ray tracing. Therefore, daylight factor is typically calculated by dividing the horizontal work plane illumination indoors by the horizontal illumination multiplied by 100, as below:

$$DF = 100\times \frac{E_{in}}{E_{External}} \tag{1}$$

Where; E_{in} means inside illuminance at a fixed point

$E_{External}$ outside horizontal illuminance under an overcast (CIE sky) or uniform sky (MIT OpenCourseWare 2015)

Daylight Factor consists of three components:

1. Sky component (SC) - due to daylight received directly at the point from the sky
2. Externally reflected component (ERC) - due to daylight received directly at the point from external reflecting surfaces
3. Internally reflected component (IRC) - due to daylight reaching the point after one or more inter reflections from interior surfaces (MIT Open CourseWare 2015), (Figure 2).

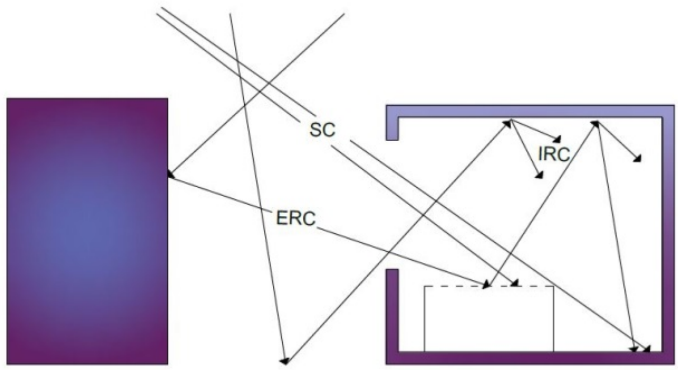

Figure 2 - Components of daylight factor

Quantitative (Numerical) and Qualitative (Visual) are two modes of evaluation for daylighting simulation in indoor environment. In the quantitative method there are 3 types of indoor illuminance; (i) experimental (scale model, full sized building, etc.), (ii) numerical (radiosity, ray tracing), and (iii) simplified (lumen, DF, etc.). In visual experiment, images are used to describe the distribution of illuminance across the work plane such as viewpoint, lighting condition and etc. In this experiment we have used the quantitative method (Papa michael et al. 2013).

1.3.3 Sky Models

As in any experiment the outcome of the simulation will be highly affected by assumptions relating to sky illuminance distribution (Mahdavi 2008). Therefore, we will look in some detail at the development of sky models.

The sun is the source of all natural daylight. Scattering of sunlight in the atmosphere by air, dust and water vapor gives the sky the appearance of a self-luminous source of light. However, these factors are not taken into account in daylight modeling. Although the sky has the same shape and position, the brightness pattern of sky is quite variable due to cloud formation and movement, such that the sky brightness distribution can change in a very short time period. This is why it has been necessary to create sky average patterns, described as sky models (Mardaljevic 1999). Researchers have proposed various sky luminance distribution models for the analysis of sunlight in the environment.

The earlier exploration of luminance distribution of overcast skies was examined by (Moon and Spencer 1942). Luminance increases by a factor of three from horizon to zenith, with the distribution of luminance showing radial symmetry with respect to the zenith. Their study was adopted by the International Commission on Illuminance (CIE) as the standard for the luminance overcast-sky. The CIE Standard overcast sky is similar to a drastically dark sky covered with thick clouds, which is the primary CIE standard sky with non-uniform luminance distribution (CIE 1955).

The luminance distribution of the clear sky model was proposed by Kittler (1967), which is the model adopted as the CIE standard for clear sky (Kittler 1973). The CIE standard for clear sky represents near luminance distribution of a completely bright sky.

The extreme sky conditions, ranging from completely cloudy to clear sky, were shown in CIE standard skies. The luminance distribution frequency of incident for both CIE standard skies was small, since in reality most sky conditions lie somewhere in between these two extremes. Therefore, the need for a more detailed representation of the real skies was essential. During 1955 to 1994, the CIE standard overcast skies and CIE standard clear skies were enhanced and reported in a number of journals (Tregenza et al. 1994) and an additional intermediate standard sky was created (Nakamura et al. 1985). This standard sky model includes the description of the distribution of the intermediate sky luminance, through classifying sky conditions into overcast, clear and intermediate. An equation related to the zenith luminance of the intermediate sky was proposed at the same time. This model is an average sky model of each solar altitude of all the skies, except for the ones similar to the two CIE Standard Skies (Igawa et al. 1997).

Additionally, a sky luminance distribution model for each solar altitude called “BRE Average Sky” was proposed by Littlefair (1981). In this model the ‘average sky’ (based on measurements for a wide range of real skies) is recommended, instead of CIE overcast sky. “BRE Average Sky” was based on the measurement data produced by Wegner in 1975. This model can be used to predict average indoor luminous or to estimate energy savings achieved. However, the limitations of this model is that it is primarily suitable for specific areas in the world, such as the south of England (Roy et al. 1995).

Later on, the sky was categorized into 5 different types by Perraudeau (1988). Basic equations for sky luminance distribution with adjustable coefficients were expressed in this model. These categories are overcast sky, intermediate overcast sky, intermediate sky, intermediate clear sky and clear sky (Roy et al. 1995).

More recently, an all-weather model was proposed by Perez et al. (1993). This model categorized the sky in "CIE clear sky model" into eight types, and includes options to control the luminance distribution through a set of three factors to reflect the conditions as; (i) sky clearness, (ii) sky brightness, and (iii) solar elevation. These three parameters are influenced by the ratio of normal to diffuse incident radiation. However, this classification has subsequently been further developed into a further fifteen categories based on additional factors, and other researchers have offered even more sky luminance models since then Igawa et al. (1997), Lam et al. (1997) and Mardaljevic (1995).

For instance, the ASRC-CIE model is linear combination of four skies – (i) the CIE clear sky or Killter clear sky, (ii) the Gusev Turbid clear sky, (iii) the intermediate sky and (iv) the CIE overcast sky. In this model the coefficients of linear combination are calculated using two factors; sky clearness and sky brightness (Littlefair 1994).

Another model is the Matsuura intermediate sky model, which was formulated to reproduce luminance patterns for specific conditions. The sky conditions used here were; (i) with thin clouds (ii) with sun (intermediate) and (iii) clear (Mardaljevic 1995).

However in Brunger's model, parameters of the insolation conditions are set as functions of the ratio of global to extraterrestrial irradiance in order to describe the sky luminance distribution. Brunger (1987) represented the sky Radiance distribution as the combined effect of two components (first being the viewing angle from zenith and second the scattering angle).

Kittler's model, the Kittler homogeneous sky, uses the illuminance turbidity coefficient, derived from direct illuminance data (Darula and Kittler 2002). It simulates the diffusion characteristics of a real sky by an equivalent homogeneous sky and has had reported success in modeling resultant horizontal illuminances, particularly for extreme conditions.

Finally, the Perez all weather sky model (Perez et al. 1993), the CIE general sky standard (Darula and Kittler 2002) and the all sky model (Igawa et al. 1997) all show detailed sky luminance distribution. These models incorporate other factors such as sky clearness and sky brightness; diffuse direct components of the solar radiation, sun position and zenith luminance (Chamaidi 2009).

1.3.4 Radiance Simulation Engine

One of the most widely used tools in daylighting simulation is Radiance; this program was developed by Ward from the Lawrence Berkeley Laboratory in California, as well as the Ecole Polytechnique Federale de Lausanne in Switzerland. From a humble beginning as a study in ray-tracing algorithms, it developed into an energy saving tool through visualization and evaluation for better lighting design, and received state funding from both the US and Switzerland. The first software, which was free, was released in 1989, and has increasingly become popular amongst architects to predict visual quality, illumination and appearance of innovative design for space, and by researchers to evaluate daylighting technology and simulation (Ward 1994).

Another important development in the widespread use of Radiance occurred when the software was chosen by the International Energy Agency (IEA) for its daylight-modeling task (Compagnon et al. 1993).

In addition, subsequent researchers such as Mardaljevic (1999), and Compagnon et al. (1993) have verified and validated daylight simulation with Radiance under a range of sky conditions and building geometries. The important attribute of Radiance is its flexibility, and there has been extensive validation of the program through comparison with physical architectural spaces (Galasiu and Atif 2002; Ng et al. 2001), controlled environments (Jones and Reinhart 2014; Mardaljevic 2001; Ng et al. 2001; Reinhart and Andersen 2006; Reinhart and Herkel 2000; Reinhart and Walkenhorst 2001) and specific material properties (Reinhart and Andersen 2006) .

There are numerous ray tracers available in the market, since the fundamental principle is relatively simple to implement on computers. A number of building performance tools use Radiance as their simulation engine. Radiance uses a backward raytracing engine, where primary rays are emitted from a point of origin (a virtual camera or illuminance sensor) to a sample of the environment. When a ray hits the surface, depending on the material of the surface, it sends out new rays. The results are combined into a single value that is the parent ray's result (Whitted 2005). Figure 3 shows components needed for rendering in Radiance (Ward 1994).

As Radiance is based on the backward ray-tracing algorithm, the light rays are traced in the opposite direction to that from which they naturally follow. The process starts from the eye (the viewpoint) and then traces the rays up to the light sources, taking into account all physical interactions (reflection, refraction) with the surfaces of the objects composing the scene. Polarization of light rays is not taken into account (Antonutto and McNeil 2006).

The great advantage of Radiance over daylighting calculation and rendering tools is that since there are no limitations for the geometry or the materials, they could be more easily simulated. Radiance uses input data to specify the scene, including geometry, materials, time and date and sky conditions. Calculated values include;

- Spectral Radiance (i.e. luminance + color)
- Irradiance (illuminance + color)
- Glare indices

Simulation results could be presented as color images, numerical values or contour plots (Dubois et al. 2003).

In this project I have chosen the Radiance program, which uses ray tracing for rendering, which could handle specular reflections well. Consequently, the preliminary results such as illuminance and luminance could be achieved. The next step is the calculation and production of simulation outcome. This is final step in the daylight simulation program.

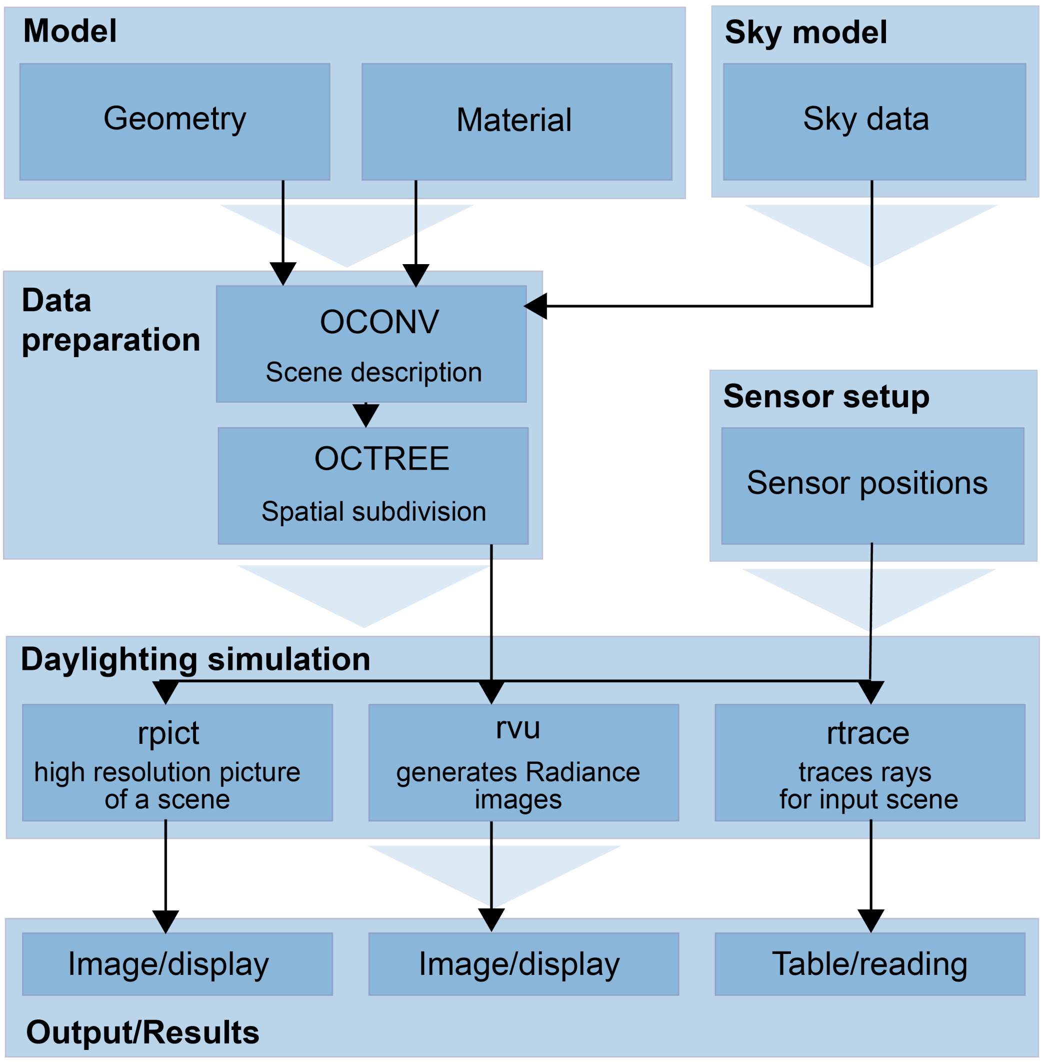

Figure 3 - components of Radiance rendering system

2 METHODOLOGY

2.1 Overview

The objective of this project is to compare the performance of various sky models by predicting the vertical irradiance on outside surfaces of a building, as well as the horizontal and vertical illuminance levels on a room's interior surfaces. The aim is to check the relative performance of the three models; SC, Gensky and Gendaylit, compared with the measurement produced by sensors. In this thesis, illuminance estimations are compared with measurements taken in an actual space in Vienna, under real sky conditions. The methodology overview is shown in figure 4.

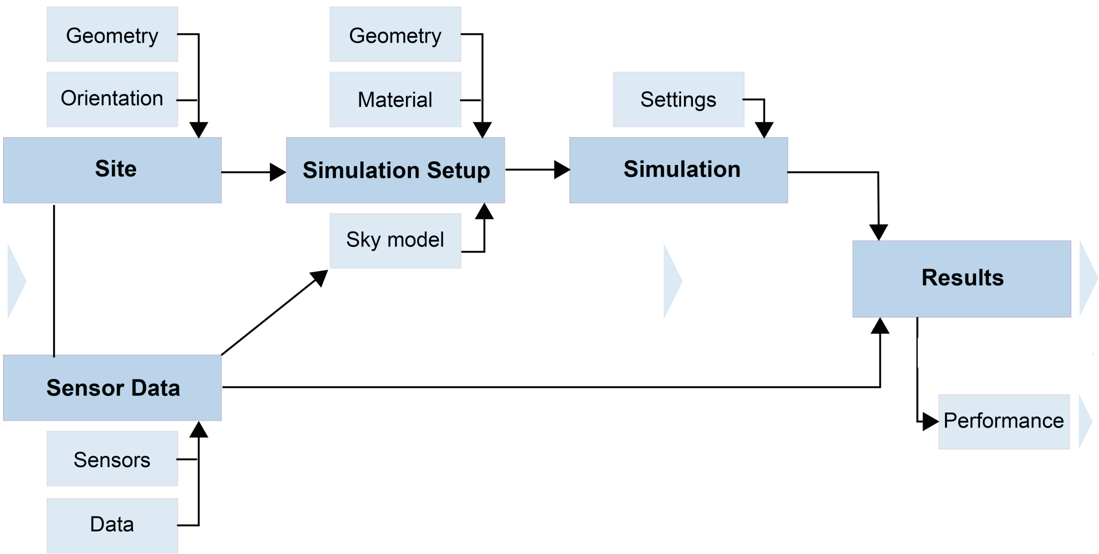

Figure 4 - Methodology overview

Eight positions in the room were equipped with physical sensors to measure illuminance on the work plane. For daylight simulation Radiance was used to generate sky luminance distribution patterns. Radiance is a highly accurate ray tracing software system. There are several benefits and reasons for choosing Radiance. These include visual quality, analyzing of lighting design and previous validation of the program.

In order to model daylight availability and distribution in architectural spaces, simulation tools require reliable representations of boundary conditions – typically in terms of sky luminance distribution models.

The next step will be computing work plane illuminance values for the test room, using the simulation program. Three sky models (Gensky, which created a description for a CIE standard sky distribution, Gendaylit, for a Perez standard sky distribution (Perez et al.

1993), and SC, based on measured values obtained from a sky scanner) will be compared with results recorded by sensors. In the final step, measured illuminance values by physical sensors and different simulation scenarios will be compared.

2.2 Summary of Methodology

2.2.1 Measurement

In order to create a realistic environment for daylight modeling, it was decided to use an existing room in the building. The actual daylight reading obtained from this room will serve as the basis to evaluate the accuracy of the model. Details regarding the measurements can be seen in section 3.1 and 3.2 below.

2.2.2 Simulation Setup

For the next step a reference model was established for daylighting simulation by the Radiance software. Radiance is a program used for the analysis and visualization of lighting in design, developed by the building technology program in the Lawrence Berkeley National Laboratory in Berkley, California. Radiance program itself does not provide reasonable support for adding complex control or analysis. Therefore, another software called Matlab® was selected for running the more complex analyses. This enabled us to run processes for different time steps, using different methods, and it is the quickest way to compare different models. This program allows us to run the Radiance program with different sky models and to compare the simulated results with the sensor measurements. The details regarding the simulation setup can be seen in section 3.3 below.

3 MEASUREMENTS AND SIMULATION

3.1 Site

3.1.1 Site location and Orientation

The test room is located on top floor of Building Physics and Building Ecology Institute (BPI) of Vienna University of Technology, with location latitude of 48.1986, longitude of 16.3694, and the height above sea level of 193 meters.

The site building orientation was measured by the azimuth angle of surface to the north using QGIS© program (an Open Source Geographic Information System). Using QGIS the orientation of the building was calculated as 21.30° degrees (Appendix A). However, in Google Map the orientation was calculated as 22.5° degrees (Figure 5). Therefore, to find the correct orientation angle of the building, another measurement was taken. The altitude and azimuth of the sun were used to arrive at the shadow points on the ground. The shadow, its angle and the azimuth were used to determine the orientation of the building to be 22.5°.

Figure 5 - Orientation of test room (Google Map)

3.1.2 Geometry

The test room dimensions are 8.4 meters long, 3.2 meters wide and 2.7 meters high. The test room was chosen for the following reasons:

- *A number of past research has been conducted in this room. This enabled us to have easy access to full data about the room and its location.*
- *The room was positioned near the weather station of BPI institute, allowing full access to the available data (such as GHI) from the weather station.*
- *There are no other high-rise buildings in surrounding area, allowing natural light coming through the windows without reflectance from other buildings interfering with the results.*
- *Windows were south facing, allowing maximum light through.*
- *There were no occupants in the room, hence there was no disturbance during the course of the experiments.*
- *There were a number of sensors positioned in the room for other experiments, potentially allowing access to a larger set of data.*

Aerial photos 6 and 7 below show the location of test room, its surroundings and the location of weather station at top of the building.

Figure 6 - Aerial view of test room and surroundings from above (Google Map)

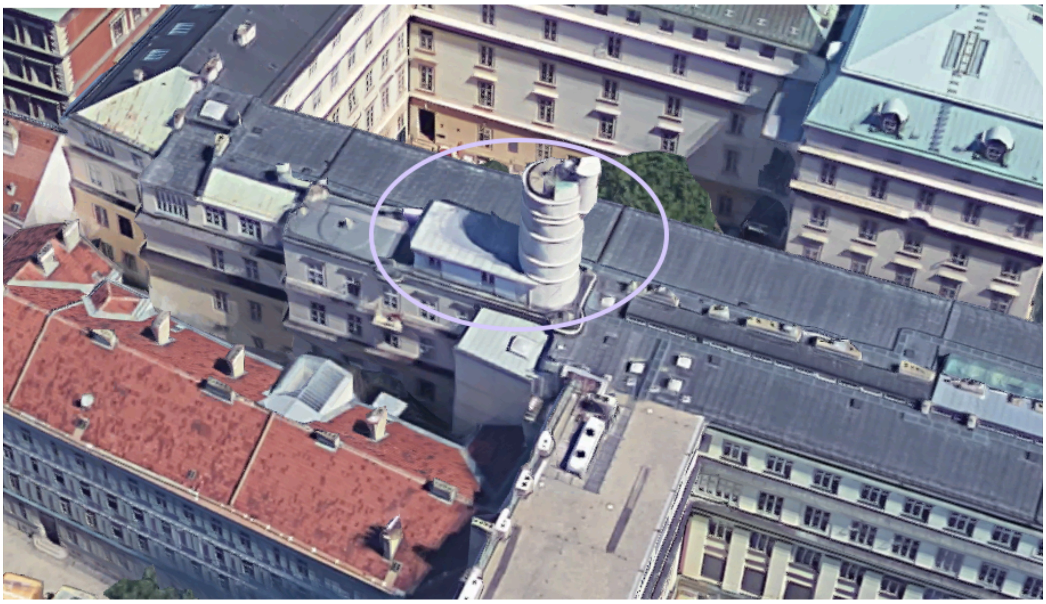

Figure 7 - Aerial view of test room and surrounding from south (Google Map)

To reduce the major sources of distortion, chairs and other furniture were removed from the room during the experiment. Therefore, the test room was empty except for three tables and one TV-set. There were two windows in the south façade allowing light entering the room. Figure 8 shows plan of the test room. Walls and ceiling were painted white, the floor was light wooden, and the tables were light grey. The surface reflectance was measured for each element (floor, wall, ceiling, tables, door and the window frames). The surface reflectance measurements were taken on three different dates and then the average of these three measurements was used. Due to the fact that illuminance measurement is sensitive towards shadows, it was necessary to prevent human movement or any other interference during the measurement.

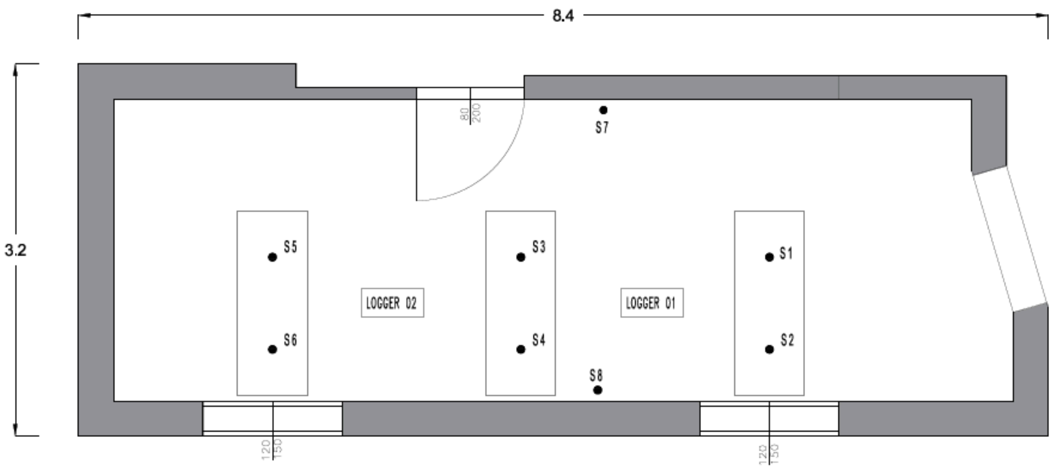

Figure 8 - Plan of test room and location of sensors

3.2 Sensors

3.2.1 Sensor Position - External and Internal

External Sensors - The Weather Station is located on the rooftop of Building Physics and Building Ecology Institute (BPI) of Vienna University of Technology. It is equipped with accurate instruments (Sunshine Pyranometer (SPN1), Shadow Ring (CM 121), Global Radiation (FLA 613 GS) etc.) measuring global and diffuse horizontal irradiance and vertical global irradiance levels for four cardinal directions. Moreover, sky scanner (MS321LR) is measuring diffuse distribution of radiance and luminance over sky hemisphere (Figure 9). The list and details of which could be found in Appendix B and C.

Internal Sensors - To measure horizontal indoor illuminance, six sensors were positioned on the table work plane, at a height of 0.74 meter. The sensors were placed in pairs along two straight lines parallel to the length of the room in such way that they divided the length of the room into 4 parts. In addition, two illuminance sensors were placed vertically near walls (one facing the windows and the other in the opposite direction) to measure vertical illuminance at a height of 1 meter. Figures 9 and 10 show the location of interior illuminance sensors in the test room.

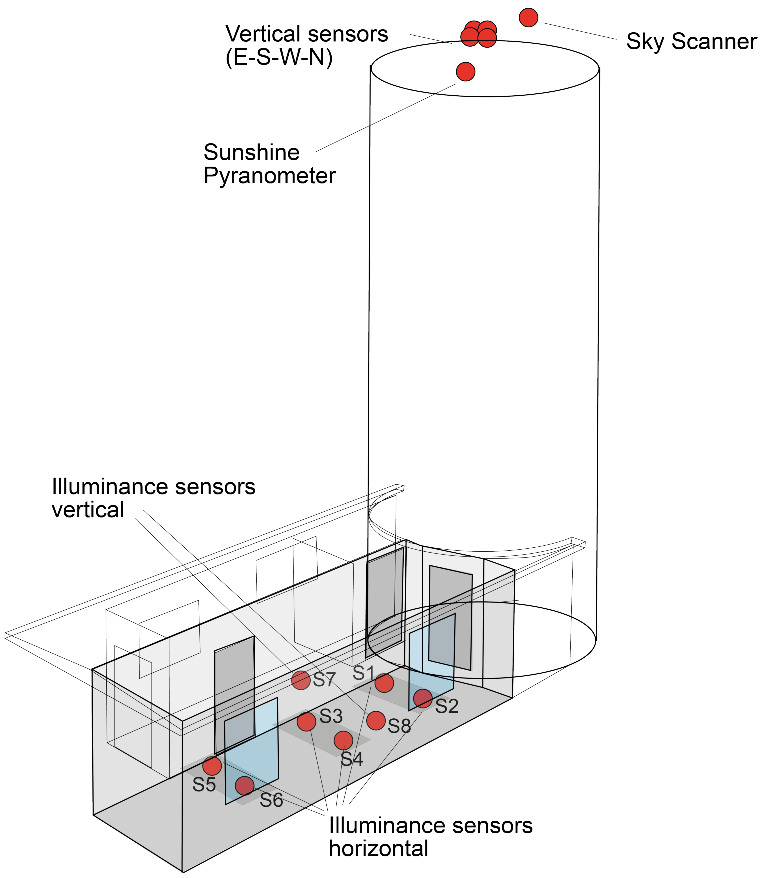

Figure 9 - Plan of test room and location of internal and external sensors

The internal illuminance sensors and data logger used in this experiment are shown in table 1.

Table 1 - Indoor Sensors

Instrument	TYPE	Measured Quantity	Units	Model Number	Manufacture
	Illuminance Sensor	Indoor illuminance	lx	CA808	Chauvin Arnoux
	Data Logger	-	-	2890-9	Almemo

Figure 10 - Position of sensors in test room

Data

The internal illuminance data was obtained as an output file. The illuminance measurements for the test room were taken at one-minute intervals. However, because of the long simulation time and the interval of data from the weather station, it was decided to use 15-minute intervals for the experiment. Each "Logger" records the data of four sensors (there were two loggers in total), containing time and illuminance measurements. The output of measured data can be presented in "List", "Column" or "Spreadsheet" formats. The output files can be processed by various spreadsheet software. In this project we used Microsoft Office Excel to present and analyze the data. An extract of Csv-format file for one day is shown in figure 11.

	A	B	M	N	O	P	Q	R	S
1									
2	ALMEMO	BEREICH:	Mess	Mess	Mess	Mess			
3	2890-9	KOMMENTAR:							
4	SD3.10	GW-MAX:							
5	ALMEMO.0	GW-MIN:	WALL West	TA W	TA E	WALL EAST			
6	DATUM:	ZEIT:	M10: lx	M11: lx	M12: lx	M13: lx			
18	24.06.15	7:37:00	1209,	1600,	2586,	676,			
19		7:38:00	1319,	1594,	2788,	786,			
20		7:39:00	1283,	1462,	2580,	734,			
21		7:40:00	1299,	1517,	2550,	746,			
22		7:41:00	1303,	1644,	2693,	783,			
23		7:42:00	1189,	1528,	2471,	696,			
24		7:43:00	1260,	1697,	2645,	780,			
25		7:44:00	1300,	1672,	2700,	786,			
26		7:45:00	1279,	1675,	2731,	768,			
27		7:46:00	1317,	1699,	2769,	782,			
28		7:47:00	1350,	1750,	2841,	793,			
29		7:48:00	1339,	1705,	2870,	782,			
30		7:49:00	1331,	1659,	2856,	770,			
31		7:50:00	1302,	1615,	2773,	742,			

Figure 11 – Sample of data format

3.2.2 Measurements, Date and Weather Type

The operation was conducted during summer and the measurements were taken on different weeks. The first test period was from 24th of June 2015 to 26th June 2015. The second set of measurements was taken during 1st July 2015 to 10th July 2015, and final measurements were from 1st September 2015 to 16th September 2015 (Table 2). From the available data three days were chosen for this experiment: 3rd July 2015 (a clear day), 5th September 2015 (an overcast day), and 7th September 2015 (an intermediate day), representing three different sky conditions.

Table 2 - Measurement periods'

Date	Time
From 24.06.2015 to 27.06.2015	7:30-17:20
From 01.07.2015 to 10.07.2015	17:00-9:20
From 01.09.2015 to 16.09.2015	17:50-12:00

The radiation reaching the earth's surface can be represented in a number of ways. Global horizontal irradiance (GHI) is the total amount of shortwave radiation received from the solar radiation by a surface horizontal to the ground. Global horizontal irradiance is the sum of diffuse radiation irradiance on a horizontal surface and the direct normal irradiance (DNI) projected onto the horizontal surface (Tregenza and Sharples 1995).

Direct normal irradiance is solar radiation in a straight line from the direction of the sun at its current position in the sky. Diffuse horizontal irradiance (DHI) is solar radiation that does not come on a direct path from the sun, but has been scattered by molecules and particles in the atmosphere and comes equally from all directions. Global horizontal irradiance (GHI) includes both direct normal irradiance and diffuse horizontal irradiance (Hiscocks 2011).

From global horizontal irradiance, diffuse horizontal irradiance and the sun zenith angle, the direct normal irradiance can be found using the following formula (Hiscocks 2011):

$$GHI = DHI + DNI \times Cosine(Solar\ Zenith\ Angle) \qquad (2)$$

The same relationship also holds for illuminance irradiance (Figure 12). The measurements of GHI and DHI are collected from the weather station on the rooftop of the BPI institute (Appendix A).

Moreover, to allow comparison of the data, parallel measurements of vertical irradiance were taken at the same location for four orientations; North, East, South and West.

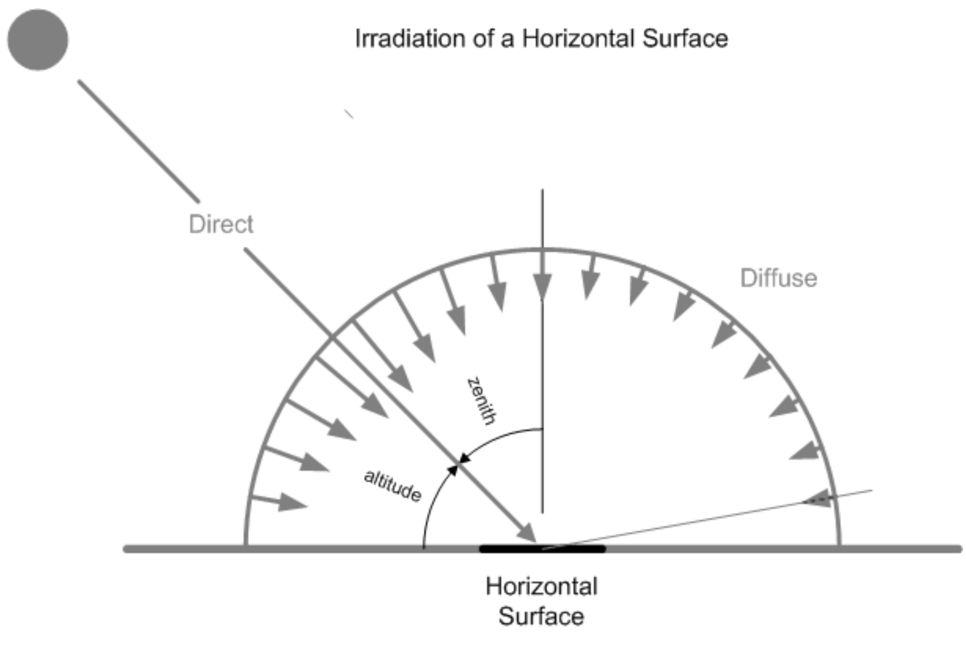

Figure 12 - Global horizontal irradiance

3.3 Simulation Setup

3.3.1 Daylight Simulation Model - Radiance

There are different tools and methods to simulate indoor illuminance conditions and related daylight indicators. In the present study, Radiance lighting simulation program was selected. The advantage of Radiance is that it has no limitation for the geometry and surface material of the building. Radiance provides a suitable algorithm, which is based on ray tracing. Radiance requires geometry, materials of the building and a sky model (See more Appendix D). Three sky models (Gensky, Gendaylit and SC) were selected for this simulation (Figure 13). Matlab® was selected to run the actual observed readings from weather station BPI for the three selected dates, as well as the real measurements obtained from the sensors, and then these were compared with the simulated predictions. These calculation steps were automated in Matlab. In the following sections the components of the daylight simulation experiment will be explained.

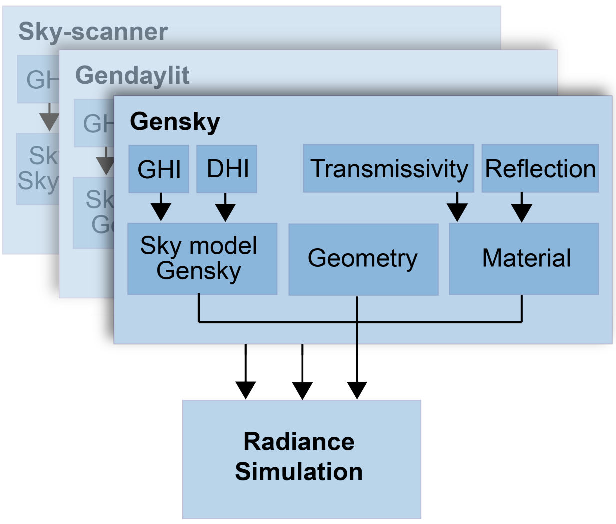

Figure 13 - Quick look Radiance simulation

3.3.2 Building Geometry

The first step in setting up the daylight environment in the model is to create the three dimensional structure of the building. The 3D model of the test room was created in SketchUp program and then with the help of the “su2ds” plug-in the geometric data from SketchUp was exported to Radiance for daylighting analysis (Bleicher 2007). The simulation model of the test room was geometrically identical to the actual test room. The dimensions of the room, the tables and windows were measured by a tape measure, with an accuracy of $\pm$1cm. The six horizontal sensors on the table were not included in the model, but in the corresponding points at +1cm above the table surface were used for horizontal Illuminance (with the table height at 74cm), the same height as the actual sensors. For the vertical illuminance the sensor points in the model were positioned at 1 meter above the floor level, again the same as the actual sensors. (See more Appendix D)

3.3.3 Building Material

For daylighting simulation in the Radiance program the material file needs the following information: (i) the material type (mirror, plastic, metal or trans), (ii) the reflectance of the material, and (iii) the roughness and specularity of the material. The reflectance used in the model was the average measurement after and before the monitoring period. For estimating the reflectance of the opaque interior surface, illuminance (lx) and luminance (cd.m^{-2}) at the specific point of each surface were measured. The equipment used for this exercise was a Minolta luminance meter LS-100. The illuminance was measured by using a Minolta T-10A illuminance meter. Table 3 shows the equipment used for this measurement.

Table 3 - Sensors used in the experiment

Manufacture	Model Number	TYPE	Measured Quantity	Units	Instrument
Minolta	LS-100	Luminance Meter	Luminance	Cd.m-2	
Minolta	T-10A	Illuminance Meter	Illuminnace	lx	

Under the right circumstance, the luminance L of a surface is related to the illuminance E and reflection ρ by Hiscocks (2011) (See Formula 3).

$$L = \frac{E\rho}{\pi}\left(\frac{candela}{meter^2}\right) \qquad (3)$$

Where,

L: is the luminance of the port in candelas per square meter

E: is the illuminance of the port in lx

ρ: is the reflectance of the white interior of the sphere

Additionally, the roughness and specularity was calculated by Colour picker from (Jacobs). Table 4 shows the surface material in the test room, the average reflectance of different surfaces calculated by sensors, surface definition in Radiance, calculated reflectance, specularity and roughness of surfaces.

Table 4 - Measured reflectivity and Radiance data in test room

Surface of test room	Actual surface Material	Red	Green	Blue	Specularity	Roughness	Reflectivity (%)	Surface Material in Radiance
Table	Sunmica (stain finish)	0.51	0.51	0.51	0.083	0.08	0.51	Plastic
Wall	Paint (Matt)	0.88	0.88	0.88	0.02	0.08	0.88	Plastic
Floor	Wood (polished)	0.43	0.43	0.43	0.03	0.43	0.43	Plastic
Radiator	Steel core	0.58	0.58	0.58	0.02	0.08	0.58	Plastic
Entrance door	Sunmica (stain finish)	0.81	0.81	0.81	0.02	0.08	0.81	Plastic
Door (Staircase)	Sunmica (stain finish)	0.88	0.88	0.88	0.02	0.08	0.88	Plastic
Ceiling	Paint (Matt)	0.88	0.88	0.88	0.02	0.08	0.88	Plastic
Window frame	Aluminum Board (Painted)	0.85	0.85	0.85	0.08	0.02	0.85	Plastic
Server Door	Aluminum Board	0.81	0.81	0.81	0.02	0.08	0.81	Plastic

Light Transmittance through the Windows

The windows were the conduits for daylighting into the room and the correct modeling of this factor was important for the experiment. The windows were the only source of daylighting in the room. Therefore, the window frames and other details were carefully modeled. The level of available light in the room can be measured by finding the light transmittance factor of the glass. In the Radiance program, glass material is defined by its transmissivity. Transmissivity is the fraction of light not absorbed in one traversal of the glass material. Glazing manufacturers normally indicate light transmittance as being the fraction of light transmitted through the glass including inter reflection. This experiment did not rely on the manufacturer’s data. In the Radiance model a single glazed window was created to avoid complications with possible errors in the modeling (Antonutto and McNeil 2006).

In order to estimate the transmission coefficient of the glazing, illuminance (lx) at indoor and outdoor glass surfaces were simultaneously measured by a luxmeter (Figure 14). Hence, the difference between illuminance values measured before and after entering the glass was calculated. This exercise was carried out several times and then the average result of transmisivity was used for the exercise in Radiance (Table 5).

Figure 14 - Test experiment to find transmissivity

Table 5 -Sample measurement of transmissivity

Dates for measuring Transmissivity of Window by lux meter	Outside Building (lx)	Inside Building (lx)	Transmissivity (%)
01.09.2015	60700	41500	68
01.09.2015	69300	53000	76
01.09.2015	65000	51500	79
14.01.2016	76800	54500	70
14.01.2016	83900	64900	77
14.01.2016	84900	66900	77

3.3.4 Sky Model

One of the steps in daylighting simulation is to generate a sky model. For the generation of sky scene distribution, an all-weather sky model (Gendaylit), CIE standard sky model (Gensky) and measured values obtained from sky scanner (SC model) are used. Figure 15 summarizes the input parameters needed for creating Gendaylit and Gensky sky models.

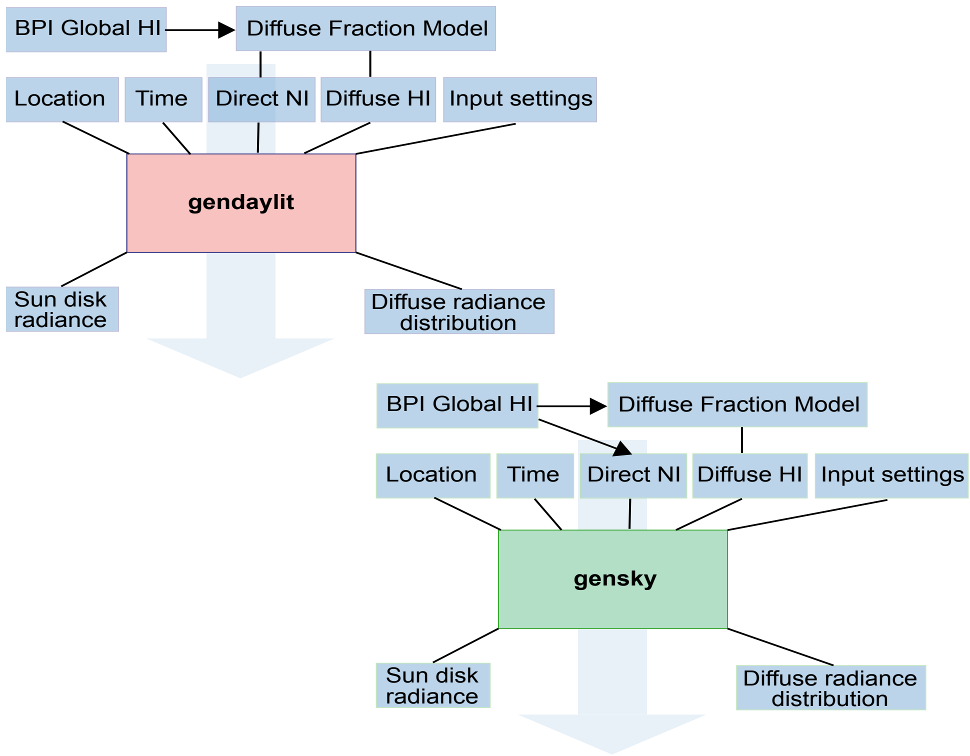

Figure 15 - Sky generations in Radiance for Gensky and Gendaylit

Gendaylit

Gendaylit is based on an all-weather sky model (Perez model) to generate a sky brightness distribution (Perez et al. 1993). The Perez model is a standard model generally used in research environment. The model allows a complete spectrum of sky in all weather conditions. The program uses the basic data including direct normal and diffuse horizontal irradiance/illuminance. This will then generate a sky luminance distribution (Ward and Shakespeare 1998). As explained previously, the weather station BPI measured the GHI and DHI. The required inputs for Gendaylit program are GHI and DNI, which are linearly related to DHI. Using the following formula we generated the sky brightness distribution data for input to Gendaylit (Formula 4).

$$DNI = \frac{(GHI - DHI)}{COS(Solar\ zenith\ angle)} \qquad (4)$$

In order to generate the sky scene description, Radiance contains two routines, Gendaylit and Gensky. These routines require, as input, information on both direct and diffuse components of solar radiation. Date, local time, angular distribution of daylight for a given atmospheric condition is used to produce a Radiance scene description. The output is the radiance of the sun and the sky integrated over the visible spectral range. The calculation for ground brightness model and sun's position can be seen in appendix E. This calculation is similar for both Gensky and Gendaylit (Delaunay 1994) .

Perez sky luminance distribution model has been used to calculate diffuse angular distribution which, quoting Perez, describes “the mean instantaneous sky luminance angular distribution patterns for all sky conditions from overcast to clear through partly cloudy skies. The normalization of the modeled sky diffuse to the measured sky diffuse irradiance/illuminance ensures the correctness of the resulting sky Radiance/luminance values in this simulation” (Perez et al. 1988).

The luminous efficacy of Perez defines the conversion of irradiance into illuminance for the direct and the diffuse components. Luminance was divided by the white light efficacy of 179 $lm.W^{-1}$ in order to convert the luminance values into radiance integrated over the visible range of the spectrum. This is in line with the Radiance calculation, as the luminance is recalculated from the radiance integrated over the visible range by:

$$luminance = (RED*.263 + GREEN*.655 + BLUE*.082) * 179 \qquad (5)$$

Radiance light sources require radiance values for red, green and blue. To calculate these values, we need to know the total initial lumen value and the total surface area of the light (Delaunay 1994).

The command used to generate Gendaylit sky model in Matlab is shown below:

```
rtrace -w -ab 5 -ad 2048 -ar 512 -aa 0.08 -as 512 -I Gendaylit_%s.oct | rcalc -e
''$1=($1*0.265+$2*0.67+$3*0.065)*179
```

Gensky

Another sky model used in Radiance program is Gensky, which produces a radiance scene description for the CIE standard sky distribution at a given month, day and time. In coding, solar angle, altitude, azimuth, GHI and DHI was used to generate the sky model. The output from sky distribution is given as a brightness function(Larson 1991)(see more in appendix E).

In the Gensky model one of the following sky options could be used:

- -s - clear sky without sun
- +s - sunny sky with sun
- -c - CIE overcast day
- -I - intermediate sky without sun
- +I - intermediate sky with sun
- -u - uniform cloudy sky

In our experiment +s for clear sky, –c for overcast sky, +I for the intermediate sky were used.

Sky scanner

In this experiment, the sky scanner (MS321LR) was installed in the Tower Room of weather station BPI. The sky scanner divided the sky dome to 145 patches (see Appendix C).This sky grid was suggested by Tregenza (1987). Maximum measuring capacity of sensors are 300 $W/m^2/sr$ for radiance and 50 $kcd.m^{-2}$ for luminance. Radiance and luminance sensors of sky scanner are not able to measure direct irradiance and luminance values respectively. Therefore, sky scanner is measuring diffuse distribution of radiance and luminance over sky hemisphere. In this experiment sky scanner's patch radiance was used. Figure 16 shows the scanning of the complete sky dome. Each patch shows the number of solar altitude and azimuth. The errors for radiance sensor were set at 0.5% for linearity. The full view angle of the scanner was 11◦. The sensitive parts of the sky scanner were contained in a weatherproof casing allowing a continuous outdoor operation.

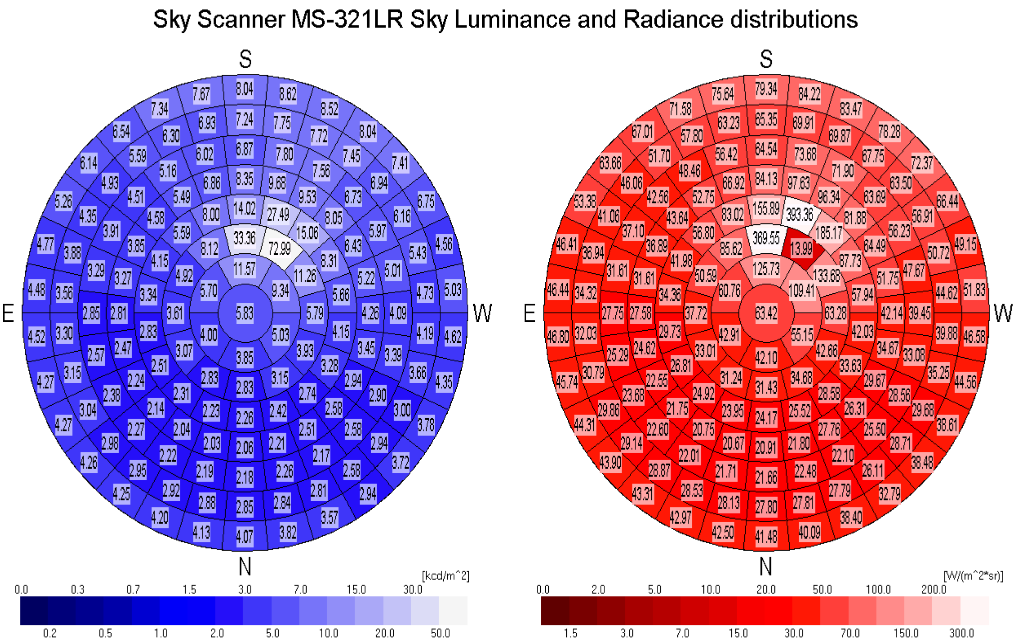

Figure 16 - Scanning sequence of 145 sky patches

Luminance Efficacy

The luminous efficacy of the global horizontal solar radiation η is defined as the ratio of the horizontal global illuminance E_v and global horizontal irradiance E_e (Formula 6).

$$\eta = \frac{E_v}{E_e}\ [lm.w^{-1}] \qquad (6)$$

The simplest way to define luminous efficacy would be to calculate a mean value from the measurements (Mahdavi and Dervishi, 2010). Luminance efficacy is the ratio of luminous to power. In Radiance, Gendaylit and Gensky derive luminance values from radiance values based on a default luminous efficacy value of 179 $lm.W^{-1}$. To maintain consistency, the same luminous efficacy value was deployed also for the SC model. However, the mean value of the measured illuminance efficacy during 2013 at our monitoring station was found to be 122 $lm.W^{-1}$.

Data Quality

In order to ensure data reliability the following filters were applied to the raw measurements in order to eliminate data distortion and outliners:

- Using shadow-ring correction to the measured horizontal diffuse data using the method described by (LeBaron et al. 1990). The shadow ring would block certain amount of the sky-diffuse components. The correction factor in our experiment for clear day is 1.14 and for overcast and intermediate is 1.10 (Appendix A).
- Only including diffuse data smaller than the corresponding global values (diffuse data should be less than the corresponding global values).
- Only including data with a solar altitude, α, greater than 5 degrees (at low altitudes, data becomes less reliable due to reflection/shading from other buildings and the cosine effect of the sensors).
- Including all data with the direct normal values (i.e., (global-diffuse)/sin α) lower than the corresponding extraterrestrial solar components (direct normal values should never be greater than the corresponding extraterrestrial solar values) (Li and Lam 2007).

3.3.5 Simulation-Ambient Parameters

To produce accurate results for daylighting, Radiance program needs a number of ambient parameters, namely; ambient bounces (-ab), ambient accuracy (-aa), ambient resolution (-ar), ambient divisions (-ad) and ambient super-samples (-as). Radiance uses these ambient parameters in the rtrace command to calculate illuminance. The actual parameters used in the program are shown in the table 6 below (Jacobs).

The command used for generating illuminance ambient parameters was:

rtrace -w -ab 5 -ad 2048 -ar 512 -aa 0.08 -as 512.

Table 6 - Parameters used for rpic rendering in Radiance for daylighting calculation

Parameters	Description	Fast	Accurate	Very Accurate
-ab	Ambient bounces	0	2	5
-aa	Ambient accuracy	0.2	0.15	0.08
-ar	Ambient resolution	32	128	512
-ad	Ambient divisions	32	512	2048
-aa	Ambient super-samples	32	256	512

In the initial stages of the experiment, “Fast” parameters to make the program faster to carry out its calculations were used. As “Fast” results are not accurate enough for daylighting purposes, “very accurate” parameters were used. Despite this making the calculations longer to conclude, the results produced were more accurate.

As described previously the test room was on the top floor of the building. In order to make the design of the building in the Radiance program simpler it was assumed that the experiment room was on the ground floor of the building, as in practice the outside ground reflection (glow) has little influence on the resulting indoor illuminance. The ground reflection was assumed to be zero.

3.4 Statistical Comparison

In order to compare the simulation and measurement results, a number of typical statistical indicators were used; Mean Bias Error (MBE), Root Mean Square Error (RMSE), Mean Absolute Error (MAE) and Percentage of Results (PR) with certain Relative Error (RE) ranges (Formula 7 , 8 , 9 and 10).

$$MBE = \frac{\sum_{i=1}^{N}(Simulated - Measured)}{N} \tag{7}$$

$$RMSD = \sqrt{\frac{\sum_{i=1}^{N}(Simulated - Measured)^2}{N}} \tag{8}$$

$$MAE = \frac{\sum_{i=1}^{N}|Simulated - Measured|}{N} \tag{9}$$

$$RE = \frac{|Simulated - Measured|}{Measured} \qquad (10)$$

N = number of observations

Additionally the cumulative distribution function (CDF) of Percentage of Error Result (PR) is produced versus discrete relative error (RE) is provided. Such graph demonstrates the percentages of results falling below a certain error level.

4 RESULTS AND DISCUSSION

4.1 Overview

This chapter summarises the main results of the experiment. It is divided into two sections. The first section (4.2) covers the performance of sky models under different weather conditions (sky types), comparing three sky models (Gendaylit, Gensky, and SC) and the measured vertical irradiance data obtained from the weather station BPI.

The second section (4.3) covers the results from the three sky models positioned indoors. It details the comparison of the average data taken from the 8 internal illuminance sensors (six horizontal and two vertical) with the results produced by the simulation carried out in the three sky models.

4.2 Performance of Sky Models in Outdoor Environment

As explained previously in methodology section, Radiance program was run using data generated by three sky models, namely “Gendaylit", "Gensky”, as well as “SC” to estimate the measurement of outside irradiance.

In order to test the performance of the three sky models (“Gendaylit", "Gensky” and “SC”), irradiance data from four vertical sensors (North, East, South and West orientation) positioned outside the building (the weather station BPI) were obtained. The Matlab program compared this data with the data obtained from the virtual external sensors in the simulation programs.

The following graphs show the simulations results for three sky types; clear, intermediate and overcast (Appendix F for more details).

4.2.1 Clear Day

For the clear day it can be seen that (for external vertical sensor facing East, South and West of the building, as well as the global horizontal sensor), the three sky models show a close approximation to the real measurements (Figure 17).

However, for the north-facing vertical sensor there are larger variations between the model results and the actual measurements during the early and latter part of the day. Since in our experiment for internal daylight simulation the windows were located on the south façade of the building, the larger variation noted above should not affect the results of our indoor tests.

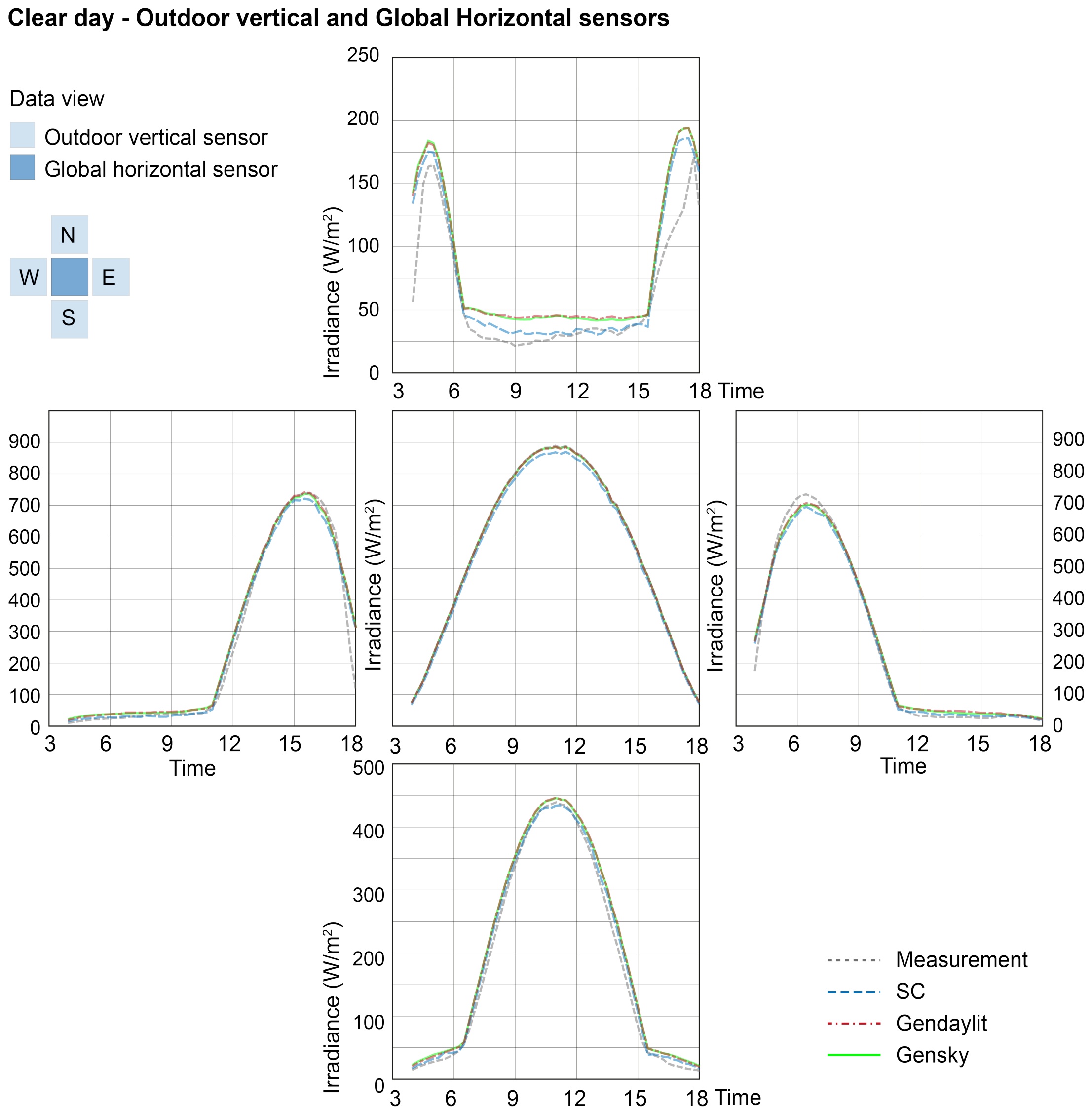

Figure 17 – Outdoor vertical and global horizontal irradiance (Clear day)

4.2.2 Overcast Day

For the overcast day it can be seen that the three sky models generally overestimate the vertical sensor value. These also show larger variations compared to the actual measurements for the vertical sensors relative to the clear day results. These variations are larger for Gendaylit (Figure 18).

For the global horizontal sensor there is an underestimation of measurements by SC and Gensky.

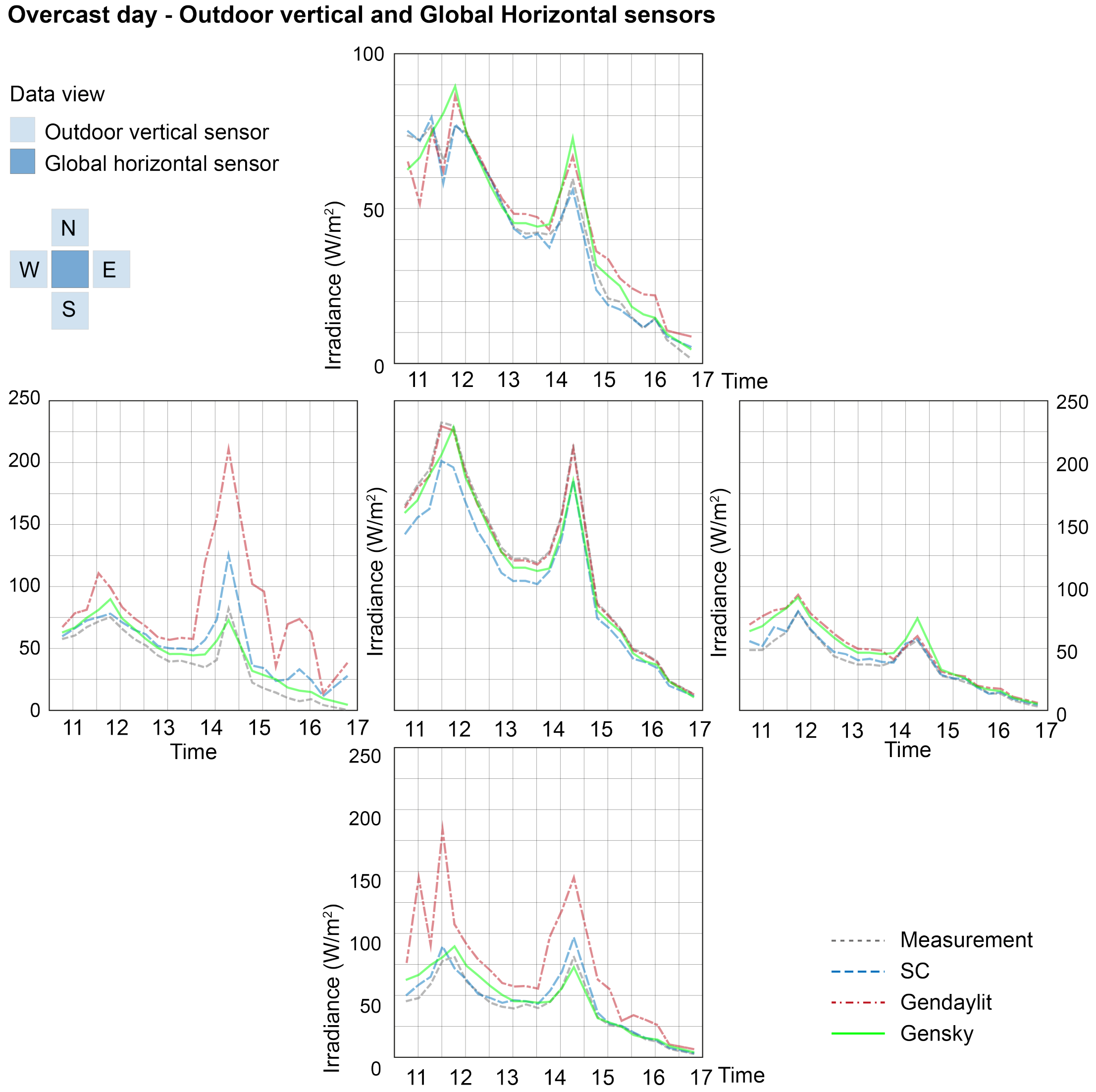

Figure 18 - Outdoor vertical and global horizontal irradiance (Overcast day)

4.2.3 Intermediate Day

For the Intermediate day, it can be seen that SC more closely predicts the actual measurements compared to the two models for the vertical sensors. For the global horizontal sensor however, SC seems to have relatively underestimated the actual measurements (Figure 19).

Intermediate day - Outdoor vertical and Global Horizontal sensors

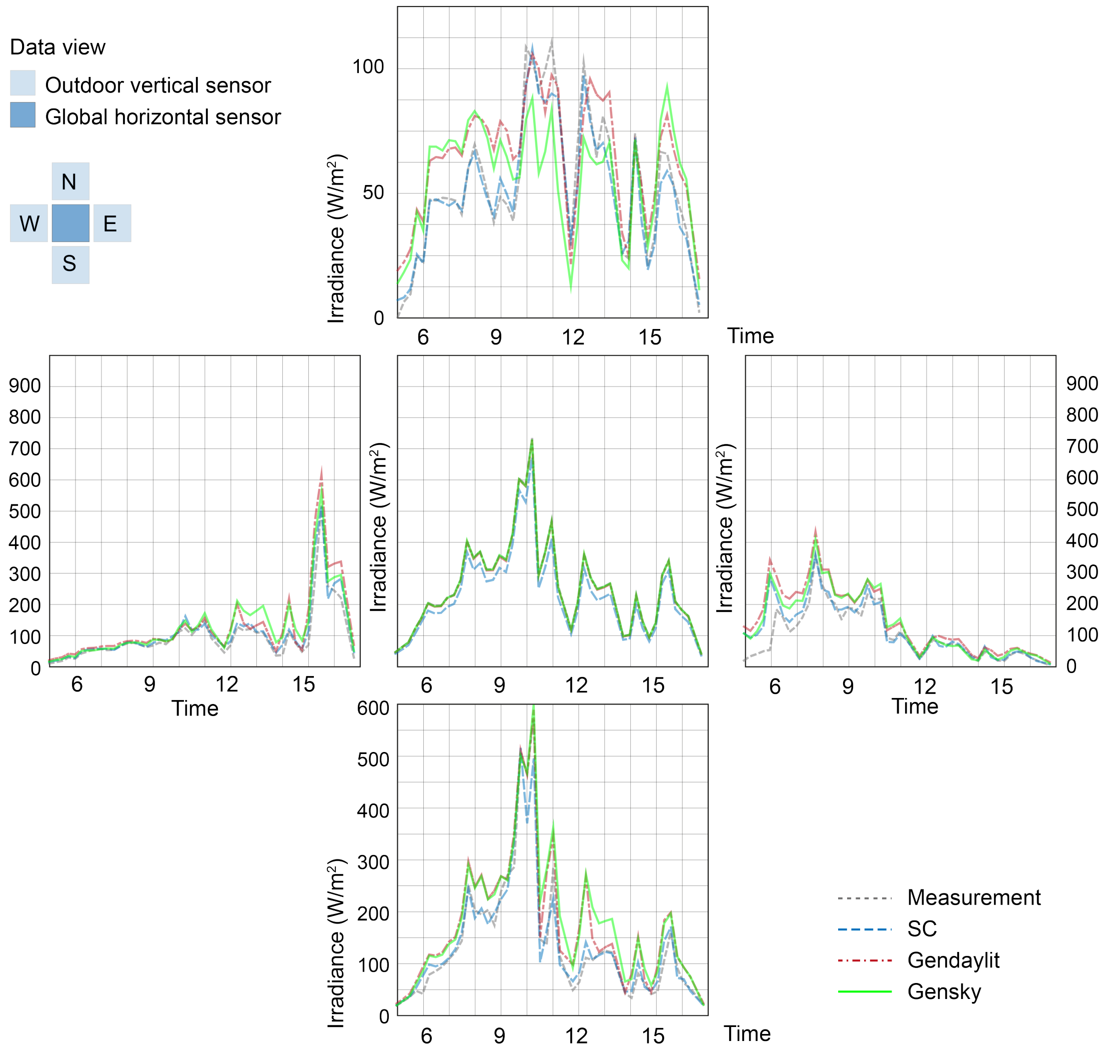

Figure 19 - Outdoor vertical and global horizontal irradiance (Intermediate day)

4.2.4 Averaging of Results for External Sensors

Figure 20 facilitates the performance comparison of the three sky models based on Cumulative Distribution Functions (CDF) of the relative errors (in ±%) for different sky conditions. The results of 130 irradiance measurements over three days (clear, overcast and intermediate weather types) have been averaged. The relative errors were grouped into North, East, South and West for vertical sensors and separately for global horizontal sensor.

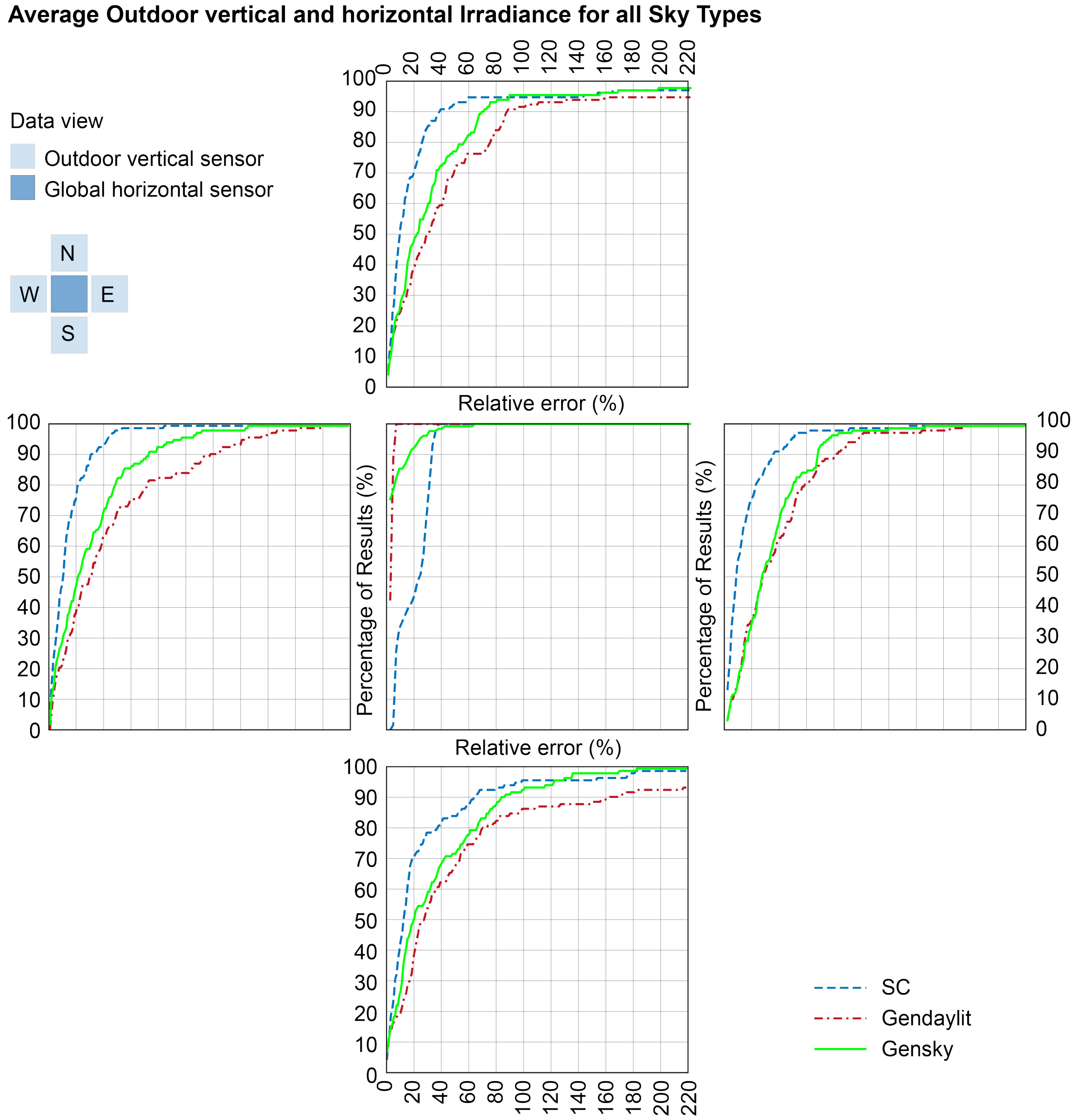

Figure 20 - The cumulative distribution function (CDF) of the relative errors for the multiple sky models

From the graph it can see that for vertical sensors SC performed most accurately, followed by Gensky and Gendaylit. For the global horizontal sensor SC seems to be marginally less accurate than the other two models. Nevertheless, all three models produced results where almost 100% of results are within a 20% margin of difference with actual readings. (Figure 20)

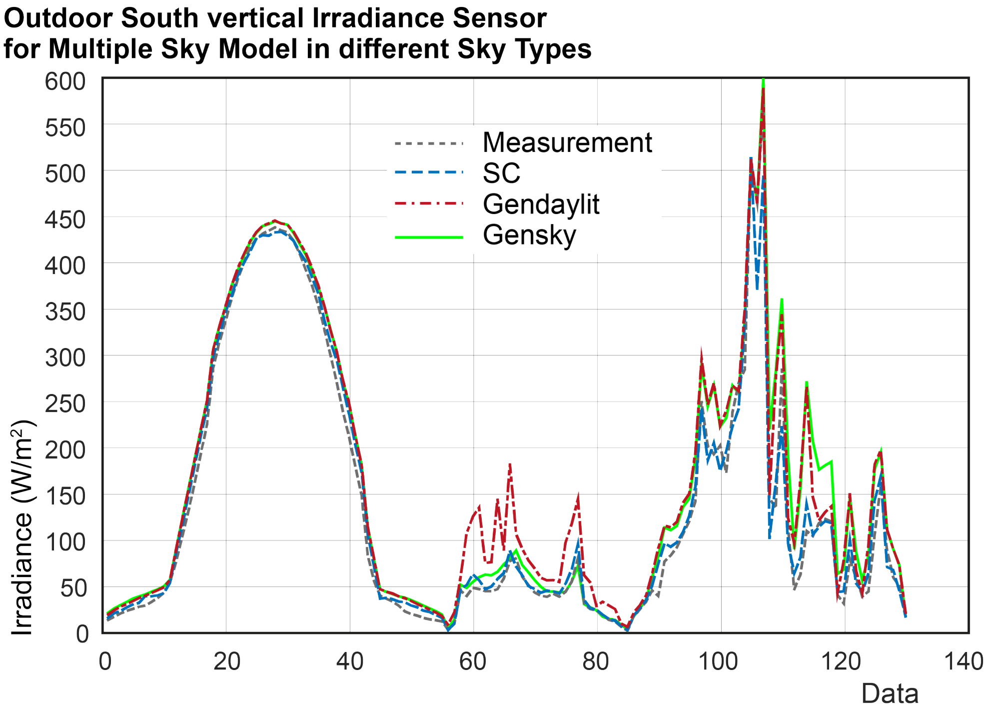

Figure 21 - South vertical irradiance sensor for different sky type

Figure 21 shows as an example of readings from one of the external sensors (south vertical). The readings are 0-55 for a clear day, 56-85 for an overcast day and 86-130 for an intermediate day. It can be seen that best predictions by all models are on the clear day. Also, it can be seen that Gendaylit shows a wider variation in results on overcast and intermediate days.

4.3 Performance of Sky Models in Indoor Environment

As previously explained sensors S2 and S6 were the only horizontal sensors positioned close to the windows, while S7 and S8 were vertical sensors. Sensors 8 and 3 are in the middle of the room and away from and not facing the windows and therefore least exposed to external light. The results from the individual sensors were compared but it was not possible to arrive at a clear conclusion about the performance of the three models based on the location of individual sensors (Appendix G). The results were therefore averaged to arrive at a more meaningful comparison in the next section.

4.3.1 Averaging of Illuminance levels for Indoor Results

The following tables and graphs summarize the error statistics (MBE, RMSE, MAE, and percentage of results with RE higher than 20%) for simulated horizontal (averaged over six sensors) and vertical (averaged over two sensors) illuminance levels under clear, overcast, and intermediate conditions respectively.

4.3.2 Clear Day

From the following table (using MBE, RMSE and MAE) it can be seen that SC generally generates better estimates for the indoor illuminance compared to the other two models for all sensors. For horizontal sensors, Gendaylit produced marginally more accurate results than Gensky. However, the Percentage of Results for Relative Error less than 20%, is higher at 55% for both Gendaylit and Gensky, and SC is clearly more accurate, as only 20% of results show errors over 20%. However, the reverse was observed for vertical sensors, where Gensky produced marginally more accurate results than Gendaylit for indoor vertical sensors. For all models the Percentage of Results for Relative Error less than 20% is showing no predictions with an error over 20% (Appendix H for more details).

Table 7 - Error statistics for horizontal and vertical indoor illuminance simulations (clear day)

	Sky model	MBE	RMSE	MAE	PR>20%RE
Horizontal	SC	4	16	14	20
	Gensky	23	26	23	55
	Gendaylit	20	24	20	55
Vertical	SC	-7	12	9	0
	Gensky	11	13	11	0
	Gendaylit	11	14	12	0

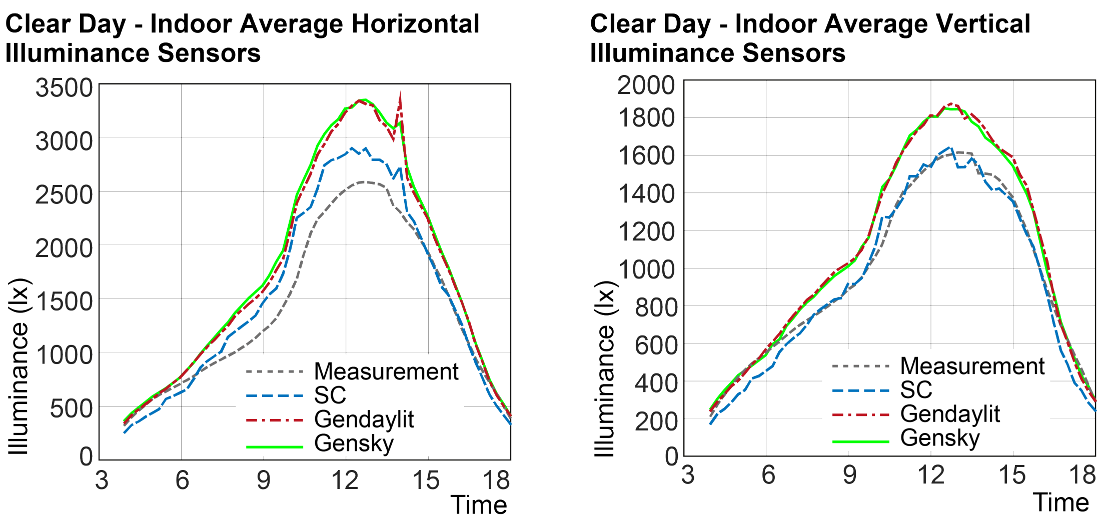

Figure 22 - indoor horizontal and vertical illuminance sensor (Clear day)

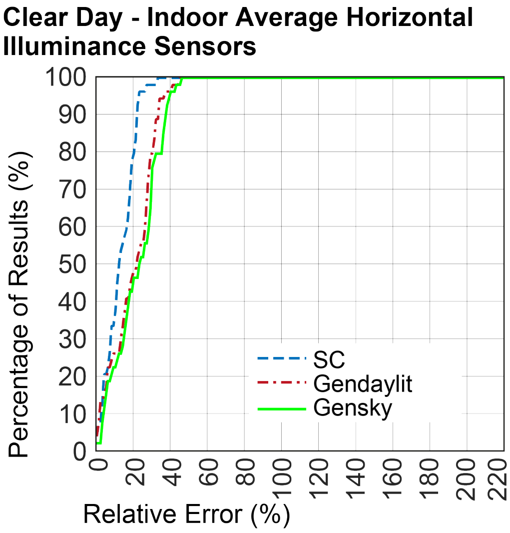

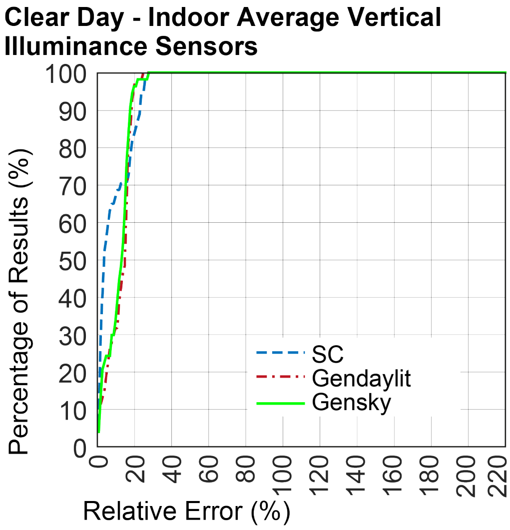

Figure 23 - Relative error to percentage of result for average indoor horizontal and vertical illuminance sensor (Clear day)

4.3.3 Overcast Day

On the overcast sky condition SC and Gensky performed more accurately than Gendaylit for both horizontal and vertical sensors. Indeed (using MBE, RMSE, MAE) the performance of SC and Gensky were very similar. However, using Percentage of Results for Relative Error less than 20%, the following can been observed: for horizontal sensors SC results showed 50% of the predictions (Gensky 90% and Gendaylit 100%) were with more than 20% error. For vertical sensors SC showed 20% (Gensky 32% and Gendaylit 100%) of results were more than 20% error (Appendix I for more details).

Table 8 - Error statistics for horizontal (S1 to S6) and vertical (S7 and S8) indoor illuminance simulations (overcast day)

	Sky model	MBE	RMSE	MAE	PR>20%RE
Horizontal	SC	30	34	30	50
	Gensky	31	35	31	90
	Gendaylit	124	136	124	100
Vertical	SC	5	15	10	20
	Gensky	13	18	16	22
	Gendaylit	132	160	132	100

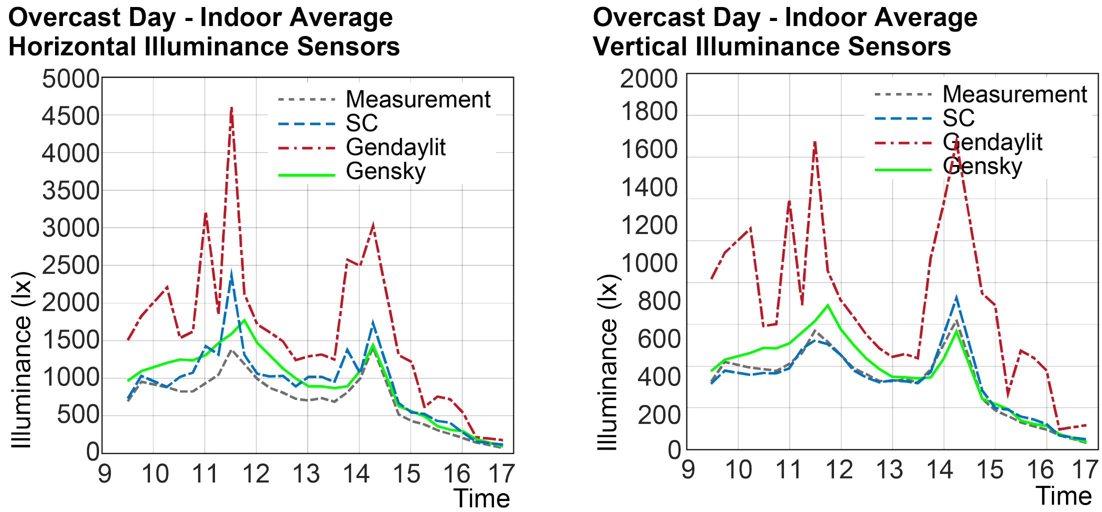

Figure 24 - Indoor Horizontal and Vertical Illuminance Sensor (Overcast Day)

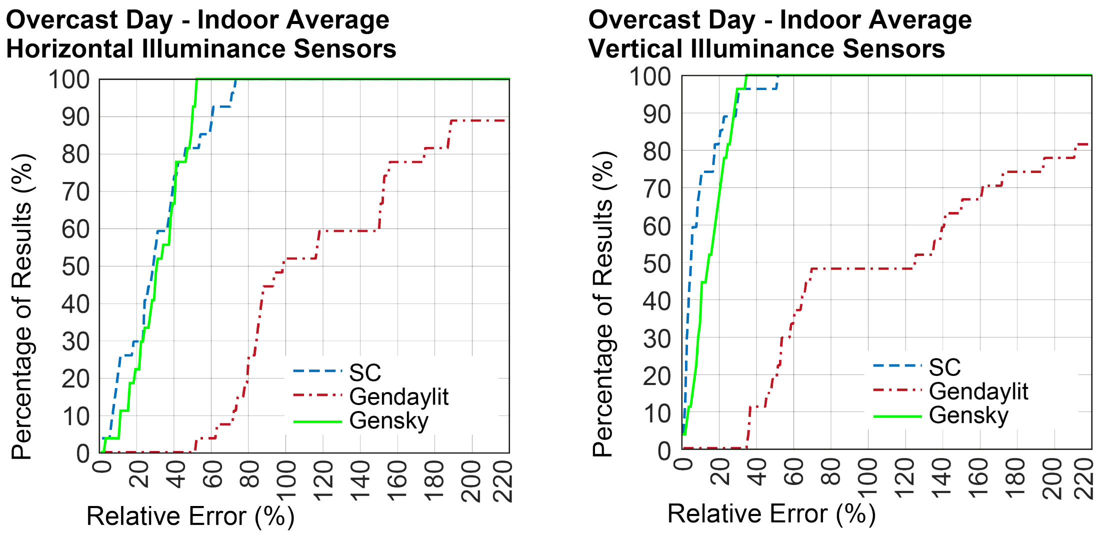

Figure 25 - Indoor horizontal and vertical illuminance sensor (Overcast day)

4.3.4 Intermediate Day

On the intermediate day SC performed better than the other two models for both vertical and horizontal sensors. It had much lower MBE/RMSE/MAE than Gensky and Gendaylit. At Percentage of Results for Relative Error less than 20% it also had a much lower percentage of 12% for vertical sensors (Gendaylit and Gensky 90%). For horizontal sensors generally the data proved to be less accurate for all three models (Appendix J for more details).

Table 9 - Error statistics for horizontal (S1 to S6) and vertical (S7 and S8) indoor illuminance simulations (intermediate day)

	Sky model	MBE	RMSE	MAE	PR>20%RE
Horizontal	SC	30	40	32	75
	Gensky	90	109	91	90
	Gendaylit	70	92	71	90
Vertical	SC	7	15	12	12
	Gensky	66	79	67	90
	Gendaylit	60	77	60	90

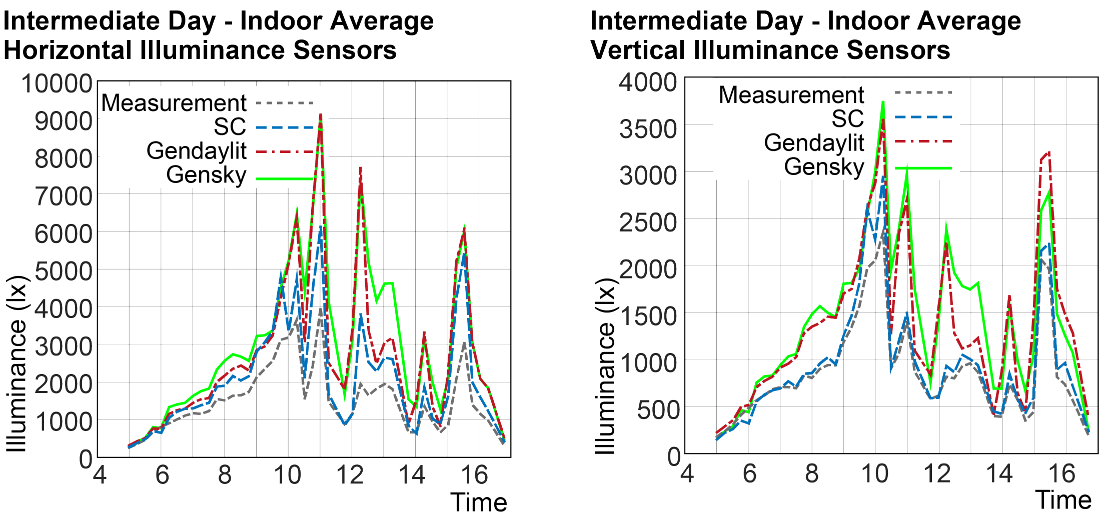

Figure 26 - Indoor Horizontal and Vertical Illuminance sensor (Intermediate Day)

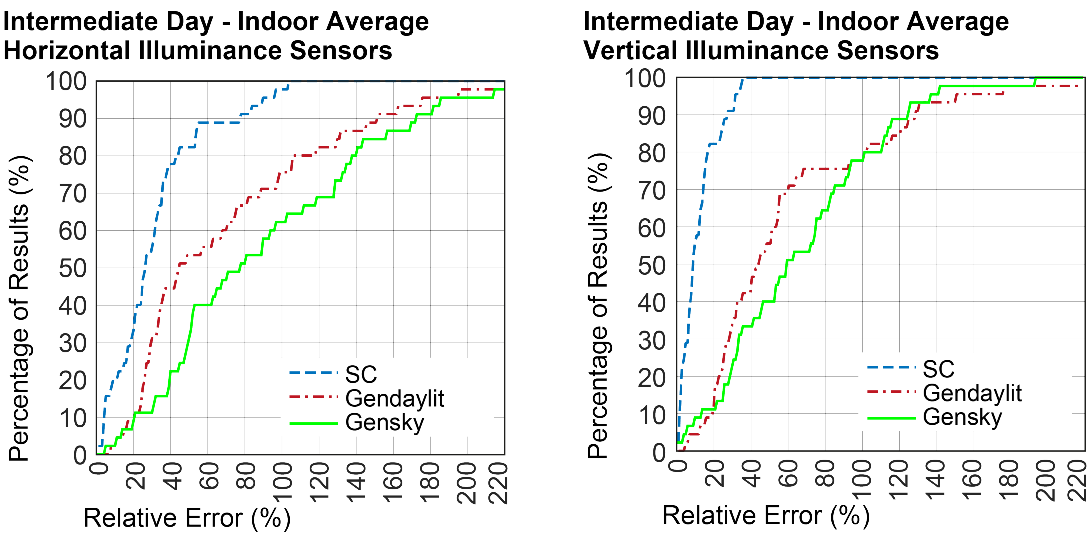

Figure 27 - Relative error to percentage of result for average indoor horizontal and vertical illuminance sensor(Intermediate day)

4.4 Summary of Result

In this experiment three sky models were evaluated by testing their performance in outdoor environment under different sky conditions. The measured data obtained by 4 external sensors was compared with the data produced by the three sky models. Although the result of the outdoor tests did not show a 100% consistent prediction, it did give a clear indication that; (a) all three sky models produced more accurate results on a clear day than either on an overcast day or on an intermediate day, and (b) SC generally performed better than Gensky or Gendaylit.

Having evaluated the three sky models in an outdoor environment, the models were then tested in an indoor environment. This was the primary purpose of our experiment, as the ultimate goal was to test the reliability of the three sky models in predicting indoor illuminance. The indoor test results showed that SC is the most accurate predicator of illuminance of workspace in the test room. This was expected as SC measured the actual sky luminance distribution. Gendaylit and Gensky produced mixed results depending on the sky type and whether the simulation was for vertical or horizontal sensors. This conclusion was consistent with the observation during the outdoor test.

In the following, we rank the average data taken by the 8 internal illuminance sensors (separately 6 horizontal and two vertical) with the average results computed by the three sky models in different sky types.

Two rankings of results were produced. Firstly, the results were evaluated by comparing MBE, RMSE and MAE. Secondly, the Percentage of Results (PR) for Relative Errors less than 20% was calculated (Table 10). The first ranking (MBE, RMSE and MAE) for horizontal sensors showed SC to be the most accurate model followed by Gendaylit and Gensky. The rankings based on vertical sensors also showed SC as the most accurate model, but this time Gensky and Gendaylit performed equally but below SC.

The results suggest that the SC model results display the lowest errors overall. This could be expected, as we used higher resolution measured radiance values to generate this model. In most practical applications, detailed sky radiance measurements are not available, which implies the need to deploy models such as Gensky and Gendaylit. Note that the performance of the latter two models was not consistent across different sky conditions. Gendaylit performed better (1. ranking) under intermediate conditions, whereas Gensky performed better under overcast sky conditions (1. and 2. ranking). Errors were generally smaller under clear sky conditions. However, the overall performance of these models cannot be considered satisfactory, at least as far as the present case study is considered. Despite careful modeling and the availability of measured horizontal (global and diffuse) irradiance value as model input, the indoor illuminance predictions displayed (for all three sky conditions) significant errors.

As mentioned before, the default luminance efficacy in Radiance does not match the actual – measured - values. Assuming that accurate values of luminance efficacy would be available for a specific location, they could be applied. In our case, the use of the measured luminance efficacy would improve the performance of the Gensky and Gendaylit models (See appendix K).

Table 10 - Relative performance (ranking) of the three Sky models in prediction of indoor horizontal and vertical illuminance under different sky condition

	Sky model	Clear	Overcast	Intermediate	1. Ranking	2. Ranking
Horizontal	SC	1	1	1	1	1
	Gensky	3	2	3	3	2
	Gendaylit	2	3	2	2	3
Vertical	SC	1	1	1	1	1
	Gensky	2	2	3	2	2
	Gendaylit	3	3	2	3	3

5 CONCLUSION

The importance of daylight in view of indoor environmental quality, user satisfaction, and energy efficiency is well established. Designers and engineers have been using different daylight simulation techniques in order to arrive at optimum daylight solutions. The principal goal of daylight calculation is to correctly estimate the level of natural light in a new design. In order to achieve this, there is a need for an advanced simulation program as well as a sophisticated sky model to match the local sky luminance distribution patterns. However, the impact of sky model errors on simulation-based indoor illuminance predictions has not been well documented.

The objective of this experiment was to compare the performance of different sky models to predict the vertical irradiance on outside surfaces of a building, and the horizontal and vertical illuminance levels on a room's interior surfaces. In this project the results produced by the three sky models were compared with the actual measurements obtained from the physical sensors. The sky models in Radiance were initially tested in outdoor environment. They were then tested for predicting indoor illuminance by comparing the results with the actual measurements.

We found that the SC model performed better, as expected. The results obtained using Gensky and Gendaylit displayed large errors, for both outdoor irradiance and indoor illuminance. Indoor illuminance levels could be predicted more accurately under clear sky conditions.

Multiple factors could have contributed to the observed discrepancies between measurements and calculations. Aside from possible errors in the measurements, input assumptions pertaining to model geometry and surface properties may involve errors. There could have been errors in selecting some of the parameters such as luminance efficacy. In Radiance, luminance efficacy was preset at 179 $lm.W^{-1}$, which is the factor we used in this experiment, however in reality the average luminance efficacy was found to be 122 $lm.W^{-1}$. Additional potential inaccuracies may include measurements of the reflectance of surfaces. Transmissivity of the window glass may also have been marginally incorrect, as average measurements were used for modeling purposes. Furthermore, the accuracy of the actual measurements by the sensors could also be a source of discrepancy in the results. Finally, the location, thickness and density of clouds can also significantly influence the accuracy of the simulation.

Given the limited scope of our study (a single room, relatively short measurement period), the generalization of the results might not be warranted. However, the presented case study does imply the need for careful characterization of the daylight simulation process in general and the reliability of sky luminance models in particular. Qualification of related accuracy statements and claims must be carefully approached in order to avoid providing the users with overtly simplistic expectations regarding models' fidelity and applicability.

Future studies for producing a universally reliable daylighting simulation may require a more robust sky model that achieves greater precision and consistent prediction in line with the real measurements. This may need an enhanced modeling of the real sky illuminance distribution.

6 INDEX

6.1 List of Figures

6.2 List of Tables

6.3 List of Formulas

7 LITERATURE

Antonutto, G. and McNeil, A. 2006. A Radiance Primer. *https://www.radianceonline.org/learning/tutorial/radiance-primer.pdf*. Accessed 31.05.2015.

Baker, N. and Steemers, K. 2014. Daylight design of buildings: A handbook for architects and engineers.

Bleicher, T., 2007. Plugin Su2rad. *http://www.jaloxa.eu/mirrors/curtin_radiance/sketchup.shtml*. Accessed 1.10.2015

Chamaidi, T., 2009. *Calibrated Sky Luminance Maps for Daylight Simulation*. Master Thesis: Vienna University of Technology.

Chou, C.P., 2004. The performance of daylighting with shading device in architecture design. *Tamkang Journal of Science Engineering*. Vol. 7, 205–212.

CIE, 1955. Natural daylight, Official recommendation.in: *CIE 13th Session,Committee E 3.2*,Vol 2.PP. 35-37.

Compagnon, R., Paule, B. and Scartezzini, J.L. 1993. Design of new daylighting systems using ADELINE software, *Solar Energy Architecture and Urban planning in Proceeding of the 3rd European Conference on Architecture,* Florence, Italy.

Darula, S. and Kittler, R. 2002. CIE general sky standard defining luminance distributions. in: *Proceeding of ESim* ,pp.11–13.

Delaunay, J.-J., 1994. Gendaylit manual pages. Frauenhofer Institute for Solar Energy Systems, Germany. *http://radsite. lbl. gov/radiance/pub/generators/index.html.* Accessed 02.11.2015.

Dubois, M.C., Grau, K., Traberg-Borup, S. and Johnsen, K. 2003. Impact of three window configurations on daylight condition.simulation with Radiance. *By og Byg documentation 047*. Danish Building and Urban Research.

Edwards, L. and Torcellini, P.A. 2002. A literature review of the effects of natural light on building occupants. National Renewable Energy Laboratory Golden, CO.

European Commission, 2009. Low energy building systems control methods in the lighting and shading domain. Brussels.

Franta, G. and Anstead, K. 1994. Daylighting offers great opportunities. Window & Door Specifier-Design Lab, pp. 40–43.

Galasiu, A.D. and Atif, M.R. 2002. Applicability of daylighting computer modeling in real case studies: comparison between measured and simulated daylight availability and lighting consumption. *Building and Environment (*37), pp. 363–377.

GoogleMap,*https://www.google.at/maps/place/Hauptgeb%C3%A4ude,+1040+Wien/@48.1986225,16.369222,31m/data=!3m1!1e3!4m16!1m10!4m9!1m3!2m2!1d16.3692722!2d48.1986983!1m3!2m2!1d16.3689062!2d48.1989988!3e0!3m4!1s0x476d0782e4dd7ca5*, Accessed 12.6.2016.

Hiscocks, P.D., 2011. Measuring Luminance with a digital camera. Syscomp Electronic Design Limited.

Holick, M.F., 2010. Vitamin D: extraskeletal health. *Endocrinology and Metabolism Clinics of North America* (39), pp. 381–400.

Igawa, N., Nakamura, H., Matsuzawa, T., Koga, Y., Goto, K. and Kojo, S. 1997. Sky luminance distribution between two CIE Standard Skies (Part 2). Numerical equation for relative sky luminance distributions.in: Proceeding of 3rd LUX ,Pacifica'97. pp. E13-E18.

International Commission on Illumination, 1970. CIE 016-1970 Daylight. ISBN 978 3 901906 664.

Jacobs,A.,2015.Radiance.http://www.jaloxa.eu/resources/radiance/documentation/docs/radiance_tutorial.pdf . Accessed 20.6.2015.

Jones, N. and Reinhart, C. 2014. Irradiance caching for global illumination calculation on graphics hardware, in: *IBPSA-USA Building Simulation Conference*, ASHRAE, Atlanta, Georgia.

Kensek, K. and Suk, J.Y. 2011. Daylight Factor (overcast sky) versus Daylight Availability (clear sky) in Computer-based Daylighting Simulations. In: *Journal of Creative Sustainable Architecture & Built Environment (1).*

Kittler, R., 1973.Standardization of luminance distribution on clear skies. CIE publication (22).

Kittler, R., 1967. Standardization of outdoor conditions for the calculation of daylight factor with clear skies, in: *CIE Intercessional Conference on Sunlight and Buildings*. pp. 273–286.

Lam, K.P., Mahdavi, A. and Pal, V. 1997. The implications of sky model selection for the prediction of daylight distribution in architectural spaces, in: *Proceedings of The 5th International IBPSA Conference*. Prague Czech Republic.

Larson, C.,1991. User's Manual DRAFT. *http://radsite.lbl.gov/radiance/refer/usman1.pdf*. Accessed 31.05.2015.

LeBaron, B.A., Michalsky, J.J. and Perez, R. 1990. A simple procedure for correcting shadowband data for all sky conditions. *Solar Energy* (44), pp. 249–256.

Leslie, R.P., 2003. Capturing the daylight dividend in buildings: why and how?, *Building Environment* (38), pp. 381–385.

Li, D.H. and Lam, T.N. 2007. Determining the optimum tilt angle and orientation for solar energy collection based on measured solar radiance data. *International Journal of Photoenergy*.

Littlefair, P.J., 1994. A comparison of sky luminance models with measured data from Garston, United Kingdom. *Solar Energy* (53), pp. 315–322.

Littlefair, P.J., 1981. The luminance distribution of an average sky. *Lighting Research and Technology (13)*, pp. 192–198.

Luo, C., 1998. To Capture the Sun and Sky "Lighting Futures", New York: Rensselaer Polytechnic Institute Lighting Research Center (1).

Mahdavi, A., 2008. Predictive simulation-based lighting and shading systems control in buildings, *Building Simulation*, pp. 25–35.

Mahdavi, A., 2005. Space, Time, Mind: Toward an Architecture of Sentient Buildings. Computer Aided Architectural Design Futures 2005, in: *Proceedings of the 11th International CAAD Futures Conference*, printed in the Netherlands. pp. 23-40.

Mahdavi, A., 2001. Simulation-based control of building systems operation. *Building Environment* (36), pp. 789–796.

Mahdavi, A., Chang, S. and Pal, V. 1999. Simulation-based integration of contextual forces into building systems control, in: *Proceedings of Building Simulation.* Citeseer, pp. 193–199.

Mahdavi, A. and Dervishi, S. 2010. Approaches to computing irradiance on building surfaces. *Journal of Building Performance Simulation* (3), pp. 129–134.

Mahdavi, A. and Dervishi, S. 2010. An empirically-based global luminous efficacy model for Vienna, Austria. Internal Report Department of Building Physics and Building Ecology.

Mardaljevic, J., 2001. The BRE-IDMP dataset: a new benchmark for the validation of illuminance prediction techniques. *Lighting Research and Technology* (33), pp. 117–134.

Mardaljevic, J., 1999. Daylight simulation: validation, sky models and daylight coefficients. PhD Dissertation: De Montfort University.

Mardaljevic, J., 1995. Validation of a lighting simulation program under real sky conditions. *Lighting research and Technology* (27), pp. 181–188.

Matlab®, Matrix laboratory. *http://de.mathworks.com/products/simulink*. Accessed - 2.06.2015.

MIT OpenCourseWare, 2015. http://ocw.mit.edu/courses/architecture/4-430-daylighting-spring-2012/lecture-notes/MIT4_430S12_lec09.pdf. Accessed 5.3.2016.

Moon, P. and Spencer, D.E. 1942. Illumination from a non-uniform sky. *Illuminating Engineering* (37), pp. 707–726.

Nakamura, H., Oki, M., Hayashi, Y., 1985. Luminance distribution of intermediate sky. *Journal of Light & Visual Environment* (9), pp. 6–13.

National Association of Rooflight manufacture, 2015. An introduction to natural daylight design in domestic properties.

Ng, E.Y.-Y., Poh, L.K., Wei, W. and Nagakura, T. 2001. Advanced lighting simulation in architectural design in the tropics. *Automation Construction* 10 (3), pp. 365–379.

Ott, J., 1997. Ergo Biolight Report. Ott Biolight Inc.

Pal, V. and Mahdavi, A. 1999. A comprehensive approach to modeling and evaluating the visual environment in buildings, in: *Proceedings of Building Simulation*. pp. 579–586.

Papa michael, K., Andersen, M., Ashdown, I., Bos, J., Brentrup, D., Cai, H., Correa, R., Digert, N., Ellersick, S. and Heschong, L. 2013. Recommended Practice for Daylighting Buildings. IES-Illuminating Engineering Society.

Perez, R., Seals, R. and Michalsky, J. 1993. All-weather model for sky luminance distribution—preliminary configuration and validation. *Solar Energy* (50), pp. 235–245.

Perez, R., Stewart, R., Seals, R. and Guertin, T. 1988. The development and verification of the Perez diffuse radiation model. Sandia National Labs., Albuquerque, NM (USA); State University of New York, Albany (USA). Atmospheric Sciences Research Center.

Perraudeau, M., 1988. Luminance models, in: *National Lighting Conference*, pp. 291–292.

QGIS©, Plugin: Azimuth and Distance Calculator, QGIS Python Plugins Repository. *https://hub.qgis.org/projects/azimuthdistances*. Accessed 2.4.2015

Reinhart, C.F., 2006. Tutorial on the use of daysim simulations for sustainable design. Institute for Research in Construction, National Research Council Canada. Ottawa (Ont.)

Reinhart, C.F. and Andersen, M. 2006. Development and validation of a Radiance model for a translucent panel. *Energy Building* (38), pp. 890–904.

Reinhart, C.F. and Herkel, S. 2000. The simulation of annual daylight illuminance distributions—a state-of-the-art comparison of six RADIANCE-based methods. *Energy Building (*32), pp. 167–187.

Reinhart, C.F., Mardaljevic, J. and Rogers, Z. 2006. Dynamic daylight performance metrics for sustainable building design. Leukos (3), pp. 7–31.

Reinhart, C.F. and Walkenhorst, O. 2001. Validation of dynamic RADIANCE-based daylight simulations for a test office with external blinds. *Energy Building* (33), pp. 683–697.

Robbins, C.L., 1986. "Daylighting, design and analysis", Van Nostrand Reinhold Company, NY, ISBN : 0-442-27949-3.

Roy, G.G., Ruck, N., Reid, G., Winkelmann, F.C.,and Julian, W. 1995. The Development of Modeling Strategies for Whole Sky Spectrums under Real Conditions for International Use. University of Sydney, Murdoch University, Australia, *http://gundog.lbl.gov/dirpubs/skymap_report.pdf*. Accessed 2.10.2015.

Ruck, N., Aschehoug, O., Aydinli, S., Christoffersen, J., Edmonds, I., Jakobiak, R., Kischkoweit-Lopin, M., Klinger, M., Lee, E. and Courret, G. 2000. Daylight in Buildings-A source book on daylighting systems and components. Lawrence Berkeley National Laboratory, Berkeley (USA).

SketchUp, Google SketchUp 2008. Ruby API Developer’s Guide. *http://www.sketchup.com/products/sketchup-pro*, Accessed 2.4.2015.

Tregenza, P.R., 1987. Subdivision of the sky hemisphere for luminance measurements. *Lighting Research and Technology* (19), pp. 13–14.

Tregenza, P.R. and Sharples, S. 1995. New daylight algorithm. University of Sheffield, Sheffield.

Ward, G. and Shakespeare, R. 1998. Rendering with Radiance: the art and science of lighting visualization.

Ward, G.J., 1994. The RADIANCE lighting simulation and rendering system, in: P*roceedings of the 21st Annual Conference on Computer Graphics and Interactive Techniques*. ACM, pp. 459–472.

Webb, A.R., 2006. Considerations for lighting in the built environment: Non-visual effects of light. *Energy Building* (38), pp. 721–727.

Whitted, T., 2005. An improved illumination model for shaded display, in: *ACM Siggraph 2005 Courses*.

APPENDIX

Appendix A: QGIS

QGIS (previously known as Quantum GIS) is a cross-platform free and open-source desktop geographic information system (GIS) application that provides data viewing, editing, and analysis. In this project this program was used to find orientation of the building. However, there was a marginal difference between QGIS data and Google map, therefore another test was carried out to establish the correct orientation of the building.

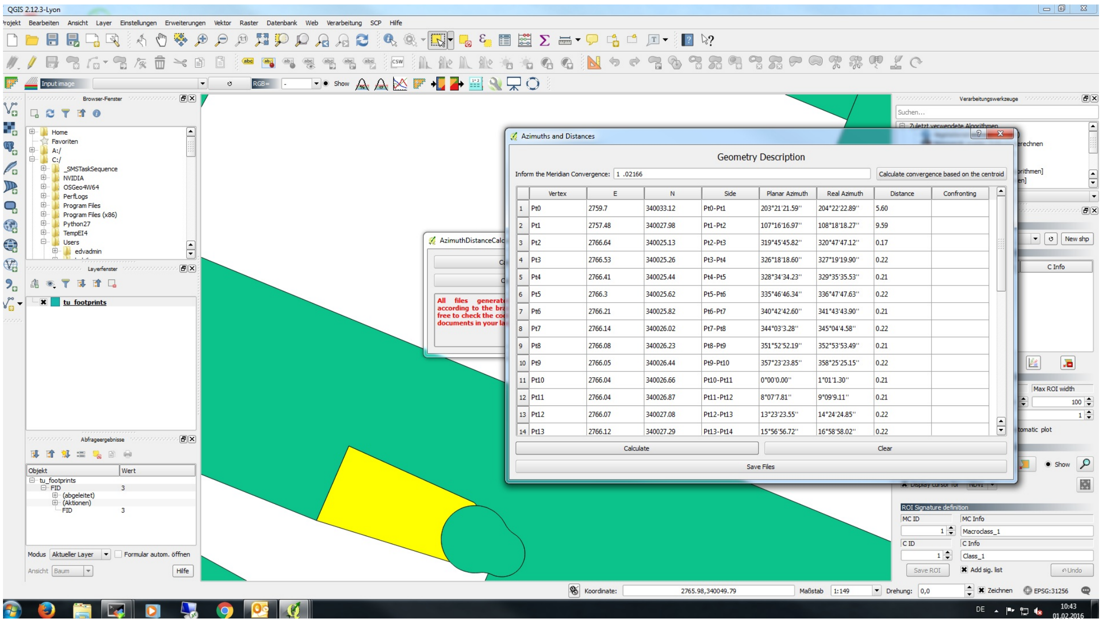

Table below shows the geographical coordinates of the test room.

MEMORIAL DESCRITIVO SINTÉTICO						
VÉRTICE	COORDENADAS		LADO	AZIMUTES		DISTÂNCIA
	E	N		PLANO	REAL	(m)
Pt0	2759.7	340033.12	Pt0-Pt1	203°21'21.59''	204°22'22.89''	5.60
Pt1	2757.48	340027.98	Pt1-Pt2	107°16'16.97''	108°18'18.27''	9.59
Pt2	2766.64	340025.13	Pt2-Pt3	319°45'45.82''	320°47'47.12''	0.17
Pt3	2766.53	340025.26	Pt3-Pt4	326°18'18.60''	327°19'19.90''	0.22
Pt4	2766.41	340025.44	Pt4-Pt5	328°34'34.23''	329°35'35.53''	0.21
Pt5	2766.3	340025.62	Pt5-Pt6	335°46'46.34''	336°47'47.63''	0.22
Pt6	2766.21	340025.82	Pt6-Pt7	340°42'42.60''	341°43'43.90''	0.21
Pt7	2766.14	340026.02	Pt7-Pt8	344°03'3.28''	345°04'4.58''	0.22
Pt8	2766.08	340026.23	Pt8-Pt9	351°52'52.19''	352°53'53.49''	0.21
Pt9	2766.05	340026.44	Pt9-Pt10	357°23'23.85''	358°25'25.15''	0.22

Appendix B: Outdoor Equipment

	SPN1-MS1 Sunshine Pyranometer
Overall accuracy: Total (Global) radiation and Diffuse radiation	±5% Daily integrals ±5% ±10 $W.m^{-2}$ Hourly averages ±8% ±10 $W.m^{-2}$ individual readings
Resolution	0.6 $W.m^{-2}$ = 0.6mV
Range	0 to >2000 $W.m^{-2}$
Analogue output sensitivity	1mV = 1 $W.m^{-2}$
Analogue output range	0-2500mV
Sunshine status threshold	200 $W.m^{-2}$ in the direct beam

	Global Radiation Probe Head FLA 613 GS
Particularly suitable for outdoor measurements	
Spectral sensitivity	400nm to 1100nm
Absolute error	< 10%
Linearity	< 1%
Operating temperature	–20°C to +60°C
Measuring range	0 to approx. 1200W/m2

	Illuminance measuring head FLA 613 VLM
Particularly suitable for outdoor measurements	
Spectral sensitivity	360 to 760 nm
Absolute error	< 10%
Linearity	< 1%
Operating temperature	–20°C to +60°C
Measuring range	0 to 170 klux (approx. 250 W/m2)

Shadow Ring (CM 121)

To be used with Kipp & Zonen pyranometers, pyrgeometers and UV radiometers to shield the instrument from direct radiation. The combination of a global measurement instrument and shadow ring CM 121 offers a simple solution to the problem of measuring diffuse radiation from the sky. The shadow from the ring covers the pyranometer dome completely. The ring will not need adjustment for several days. Naturally the ring will also intercept a small part of the diffuse radiation from the sky. Correction is necessary to compensate for this and a table of correction factors is shown below.

	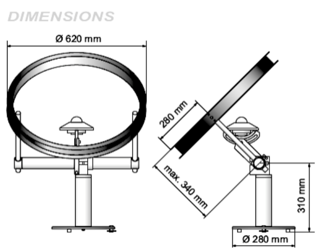
Ring width / radius rate	0.185
View angle (as seen from instrument)	10.6°
Weight, including typical instrument	6.5 KG

Table of correction factor for shadow ring:

MONTH		JAN			FEB					MAR						APR					MAY				JUN	
DAY OF MONTH		1	17	26	2	8	15	21	26	3	9	14	19	24	29	3	8	14	19	25	2	9	16	26	11	
NORTHERN LATITUDE	90	1	1	1	1	1	1	1	1	1	1	1	1	1	1.01	1.03	1.04	1.05	1.07	1.08	1.10	1.11	1.12	1.13	1.15	1.16
	85	1	1	1	1	1	1	1	1	1	1	1	1	1.01	1.02	1.03	1.04	1.05	1.07	1.08	1.09	1.11	1.12	1.13	1.15	1.16
	80	1	1	1	1	1	1	1	1	1	1.01	1.01	1.01	1.02	1.03	1.04	1.04	1.05	1.07	1.08	1.09	1.11	1.12	1.13	1.15	1.16
	75	1	1	1	1	1	1	1	1.01	1.01	1.01	1.02	1.03	1.03	1.04	1.05	1.05	1.06	1.07	1.08	1.09	1.10	1.12	1.13	1.14	1.15
	70	1	1	1	1	1	1.01	1.01	1.01	1.02	1.02	1.03	1.04	1.04	1.05	1.06	1.06	1.07	1.08	1.09	1.10	1.11	1.12	1.13	1.14	1.15
	65	1	1	1	1.01	1.01	1.01	1.02	1.02	1.03	1.03	1.04	1.05	1.05	1.06	1.07	1.07	1.08	1.09	1.10	1.10	1.11	1.12	1.13	1.13	1.14
	60	1.01	1.01	1.01	1.02	1.02	1.02	1.03	1.03	1.04	1.04	1.05	1.06	1.06	1.0	1.08	1.08	1.09	1.10	1.10	1.11	1.12	1.12	1.13	1.14	1.14
	55	1.01	1.02	1.02	1.02	1.03	1.03	1.04	1.04	1.05	1.05	1.06	1.07	1.07	1.08	1.08	1.09	1.10	1.10	1.11	1.12	1.12	1.13	1.13	1.14	1.14
	50	1.02	1.02	1.03	1.03	1.04	1.04	1.05	1.05	1.06	1.06	1.07	1.08	1.08	1.09	1.09	1.10	1.10	1.11	1.12	1.12	1.13	1.13	1.13	1.14	1.14
	45	1.03	1.03	1.04	1.04	1.05	1.05	1.06	1.06	1.07	1.07	1.08	1.09	1.09	1.10	1.10	1.11	1.11	1.12	1.12	1.13	1.13	1.13	1.14	1.14	1.14
	40	1.04	1.04	1.05	1.05	1.06	1.06	1.07	1.07	1.08	1.08	1.09	1.09	1.10	1.10	1.11	1.11	1.12	1.12	1.13	1.13	1.13	1.14	1.14	1.14	1.14
	35	1.05	1.05	1.06	1.06	1.07	1.07	1.08	1.08	1.09	1.09	1.10	1.10	1.11	1.11	1.12	1.12	1.12	1.13	1.13	1.13	1.14	114	1.14	1.14	1.14
	30	1.06	1.06	1.07	1.07	1.08	1.08	1.09	1.09	1.10	1.10	1.11	1.11	1.11	1.12	1.12	1.12	1.13	1.13	1.13	1.13	1.14	1.14	1.14	1.14	1.14
	25	1.07	1.07	1.08	1.08	1.09	1.09	1.09	1.10	1.10	1.11	1.11	1.12	1.12	1.12	1.13	1.13	1.13	1.13	1.13	1.14	1.14	1.14	1.14	1.14	1.14
	20	1.08	1.08	1.08	1.09	1.09	1.10	1.10	1.11	1.11	1.11	1.12	1.12	1.12	1.13	1.13	1.13	1.13	1.13	1.14	1.14	1.14	1.14	1.14	1.14	1.13
	15	1.08	1.09	1.09	1.10	1.10	1.11	1.11	1.11	1.12	1.12	1.12	1.13	1.12	1.13	1.13	1.13	1.13	1.13	1.13	1.13	1.13	1.13	1.13	1.13	1.13
	10	1.09	1.10	1.10	1.11	1.11	1.11	1.12	1.12	1.12	1.13	1.13	1.13	1.12	1.13	1.13	1.13	1.13	1.13	1.13	1.13	1.13	1.13	1.13	1.13	1.12
	5	1.10	1.11	1.11	1.11	1.12	1.12	1.12	1.12	1.13	1.13	1.13	1.13	1.12	1.13	1.13	1.13	1.13	1.13	1.13	1.13	1.13	1.12	1.12	1.12	1.12
EQUATOR	0	1.11	1.11	1.12	1.12	1.12	1.12	1.13	1.13	1.13	1.13	1.13	1.13	1.13	1.13	1.13	1.13	1.13	1.13	1.13	1.12	1.12	1.12	1.12	1.11	1.11
SOUTHERN LATITUDE	5	1.12	1.12	1.12	1.12	1.13	1.13	1.13	1.13	1.13	1.13	1.13	1.13	1.13	1.13	1.13	1.13	1.13	1.12	1.12	1.12	1.12	1.11	1.11	1.11	1.10
	10	1.12	1.13	1.13	1.13	1.13	1.13	1.13	1.13	1.13	1.13	1.13	1.13	1.13	1.13	1.13	1.13	1.12	1.12	1.12	1.11	1.11	1.11	1.10	1.10	1.09
	15	1.13	1.13	1.13	1.13	1.13	1.13	1.13	1.13	1.13	1.13	1.13	1.13	1.13	1.13	1.12	1.12	1.12	1.11	1.11	1.11	1.10	1.10	1.09	1.09	1.08
	20	1.13	1.13	1.13	1.14	1.14	1.14	1.14	1.13	1.13	1.13	1.13	1.13	1.12	1.12	1.12	1.11	1.11	1.11	1.10	1.10	1.09	1.09	1.08	1.08	1.08
	25	1.14	1.14	1.14	1.14	1.14	1.14	1.13	1.13	1.13	1.13	1.13	1.12	1.12	1.12	1.11	1.11	1.10	1.10	1.09	1.09	1.09	1.08	1.08	1.07	1.07
	30	1.14	1.14	1.14	1.14	1.14	1.13	1.13	1.15	1.13	1.12	1.12	1.12	1.11	1.11	1.11	1.10	1.10	1.09	1.09	1.08	1.08	1.07	1.07	1.06	1.06
	35	1.14	1.14	1.14	1.14	1.14	1.13	1.13	1.15	1.12	1.12	1.12	1.11	1.11	1.10	1.10	1.09	1.09	1.08	1.08	1.08	1.07	1.07	1.06	1.05	1.05
	40	1.14	1.14	1.14	1.14	1.13	1.13	1.13	1.12	1.12	1.11	1.11	1.10	1.10	1.09	1.09	1.08	1.08	1.07	1.07	1.06	1.06	1.05	1.05	1.04	1.04
	45	1.14	1.14	1.14	1.13	1.13	1.13	1.12	1.12	1.11	1.11	1.10	1.10	1.09	1.09	1.08	1.07	1.07	1.06	1.06	1.05	1.05	1.04	1.04	1.03	1.03
	50	1.14	1.14	1.13	1.13	1.13	1.12	1.12	1.11	1.10	1.10	1.09	1.09	1.08	1.08	1.07	1.06	1.06	1.05	1.05	1.04	1.04	1.03	1.03	1.02	1.02
	55	1.14	1.14	1.13	1.13	1.12	1.12	1.11	1.10	1.10	1.09	1.08	1.08	1.07	1.07	1.06	1.05	1.05	1.04	1.04	1.03	1.03	1.02	1.02	1.02	1.01
	60	1.14	1.14	1.13	1.12	1.12	1.11	1.10	1.10	1.09	1.08	1.08	1.07	1.06	1.06	1.05	1.04	1.04	1.03	1.03	1.02	1.02	1.02	1.01	1.01	1.01
	65	1.14	1.13	1.13	1.12	1.11	1.10	1.10	1.09	1.08	1.07	1.07	1.06	1.05	1.05	1.04	1.03	1.03	1.02	1.02	1.01	1.01	1.01	1	1	1
	70	1.15	1.14	1.13	1.13	1.11	1.10	1.09	1.08	1.07	1.06	1.06	1.05	1.04	1.04	1.03	1.02	1.02	1.01	1.01	1.01	1	1	1	1	1
	75	1.15	1.14	1.13	1.12	1.10	1.09	1.08	1.07	1.06	1.05	1.05	1.04	1.03	1.03	1.02	1.01	1.01	1.01	1	1	1	1	1	1	1
	80	1.16	1.14	1.13	1.12	1.11	1.09	1.08	1.07	1.05	1.04	1.04	1.03	1.02	1.01	1.01	1.01	1	1	1	1	1	1	1	1	1
	85	1.16	1.15	1.13	1.12	1.11	1.09	1.08	1.07	1.05	1.04	1.03	1.02	1.01	1	1	1	1	1	1	1	1	1	1	1	1
	90	1.16	1.15	1.13	1.12	1.11	1.10	1.08	1.07	1.05	1.04	1.03	1.01	1	1	1	1	1	1	1	1	1	1	1	1	1
DAY OF MONTH		12	27	18	10	4	29	23	17	12	7	1	26	21	16	11	5	31	25	19	13	6	29	19	3	
MONTH		DEC	NOV				OCT					SEPT						AUG					JUL			
SOLAR DECLINATION		-24	-22	-20	-18	-16	-14	-12	-10	-8	-6	-4	-2	0	2	4	6	8	10	12	14	16	18	20	22	24
SLIDING BAR SETTING		132	120	108	97	85	74	63	52	42	31	21	10	0	10	21	31	42	52	63	74	85	97	108	120	132

Appendix C: Sky scanner

Sky Scanner MS-321LR tracks 145 points of sky hemisphere. The sensor with aperture angle at 11 degrees and the tracker having two-axis control, measure the distribution of both luminance and radiance in 4.5 minutes.

Measurements of 145 points are based on the CIE108-1994 recommendation. Luminance value can be measured per kcd/m2 and radiance value per W/m2/sr.

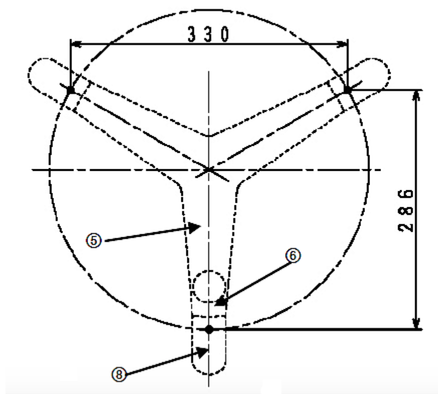

Accuracy	<0.01°
Resolution	0.009°
Size	430(W) x 380(D) x 440(H) mm
weight	Tracker: 12.5 kg
Temperture range	-40 - +50 C°

Appendix D: Test room

Test room – Radiance

The following details of the test room were computed by Radiance program based the data input.

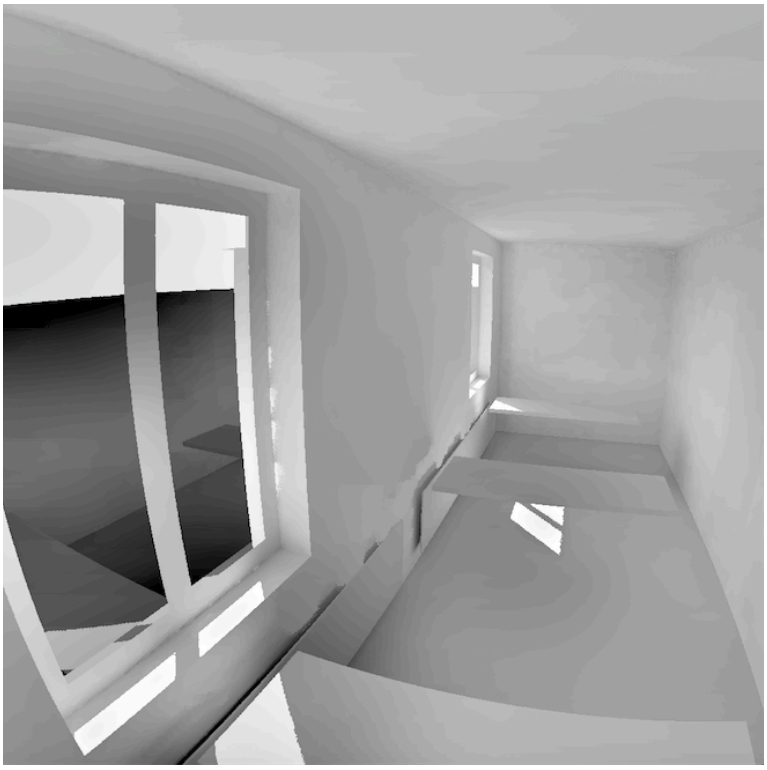

Test Room - SketchUp model

The SketchUp models of the test room was produced and then imported into Radiance program by SU2Rad. The test room is shown from different views.

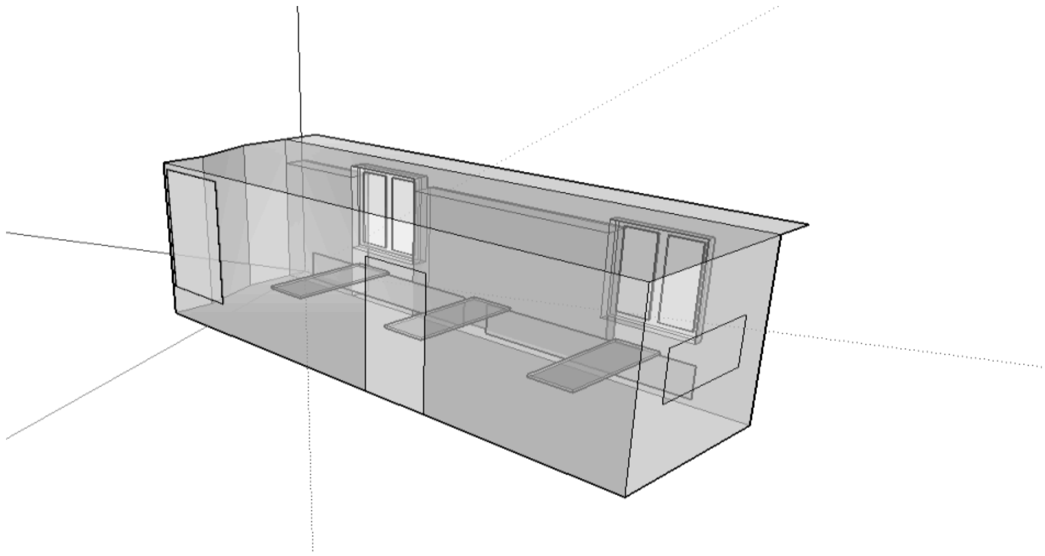

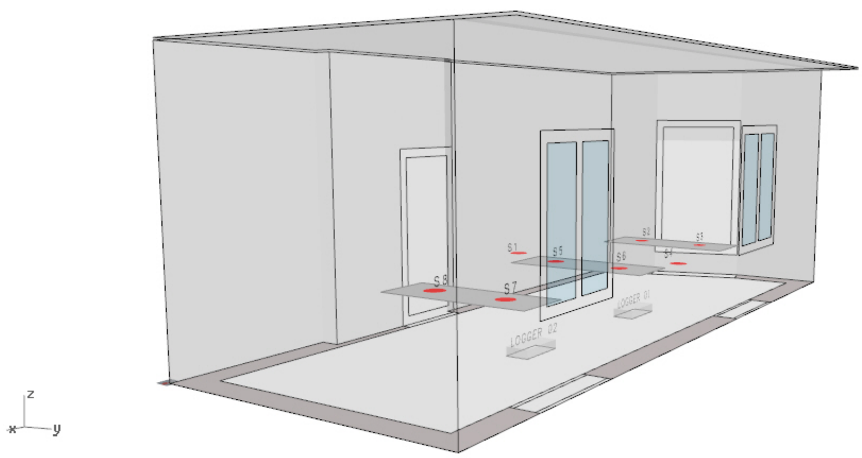

Appendix E: Sky model generated by Gendaylit and Gensky

basic glow material for sky;

brightness is defined by 'skyfunc'

skyfunc glow skyglow

0

0

4 1 1 1 0

sky dome: 'source' type with skyglow material covering upper hemisphere

skyglow source sky

0

0

4 0 0 1 180

material for ground;

skyfunc glow groundglow

0

0

4 0 0 0 0

Apply 'groundglow' to source covering the lower hemisphere

groundglow source ground

0

0

4 0 0 -1 180

Appendix F: Error statistics for outdoor irradiance simulations

The following table shows the error statistics for the three sky models in indoor environment under different sky conditions.

	Sky Model	Sky condition	North	East	South	West
MBE (%)	SC	Clear Day	19	9	12	10
		Intermediate Day	1	34	7	18
		Overcast Day	10	8	10	118
	GENSKY	Clear Day	42	24	23	32
		Intermediate Day	17	52	44	39
		Overcast Day	20	26	14	40
	GENDALYIT	Clear Day	43	27	22	31
		Intermediate Day	28	74	40	45
		Overcast Day	41	31	79	271
RMSE (%)	SC	Clear Day	30	20	19	31
		Intermediate Day	13	94	21	30
		Overcast Day	59	15	13	280
	GENSKY	Clear Day	50	37	33	50
		Intermediate Day	38	103	59	55
		Overcast Day	51	30	21	59
	GENDALYIT	Clear Day	52	44	29	47
		Intermediate Day	44	131	58	68
		Overcast Day	116	40	89	383
MAE(%)	SC	Clear Day	21	15	13	17
		Intermediate Day	9	39	15	20
		Overcast Day	17	10	10	118
	GENSKY	Clear Day	42	26	24	33
		Intermediate Day	32	54	45	39
		Overcast Day	23	26	16	41
	GENDALYIT	Clear Day	44	30	22	32
		Intermediate Day	33	74	40	45
		Overcast Day	46	31	79	271

Appendix G: Error statistics for indoor illuminance simulations

The following table shows the error statistics for the three sky models in indoor environment under different sky conditions.

	Sky Model	Sky Condition	Sensor1	Sensor2	Sensor3	Sensor4	Sensor5	Sensor6	Sensor7	Sensor8
MBE (%)	SC	*Clear Day*	7	-9	-8	-5	18	1	-6	-4
		Intermediate Day	37	1	26	-5	48	11	11	12
		Overcast Day	42	0	41	-4	54	5	9	5
	GENSKY	*Clear Day*	25	9	11	14	37	21	12	16
		Intermediate Day	95	52	75	44	111	79	74	77
		Overcast Day	36	4	8	3	49	26	19	23
	GENDALYIT	*Clear Day*	22	9	10	14	35	18	12	13
		Intermediate Day	70	46	74	40	85	57	68	57
		Overcast Day	124	105	160	96	142	106	148	108
RMSE (%)	SC	*Clear Day*	17	19	18	20	24	16	9	15
		Intermediate Day	49	18	99	12	59	17	17	22
		Overcast Day	53	20	127	18	64	11	15	18
	GENSKY	*Clear Day*	29	17	17	22	39	25	13	19
		Intermediate Day	118	64	123	54	135	96	90	93
		Overcast Day	39	11	12	10	51	29	23	27
	GENDALYIT	*Clear Day*	25	18	17	22	37	22	13	17
		Intermediate Day	95	62	134	54	110	79	87	78
		Overcast Day	136	130	248	123	157	117	178	122
MAE(%)	SC	*Clear Day*	14	14	14	16	20	14	7	12
		Intermediate Day	39	13	33	10	48	14	15	16
		Overcast Day	42	16	52	13	54	7	10	10
	GENSKY	*Clear Day*	25	15	14	18	37	21	12	17
		Intermediate Day	95	54	75	46	111	80	75	78
		Overcast Day	36	9	11	8	49	26	20	23
	GENDALYIT	*Clear Day*	22	16	15	19	35	19	12	14
		Intermediate Day	71	46	74	41	85	58	69	57
		Overcast Day	124	105	160	97	142	106	148	108
PR (%) > 20% RE	SC	*Clear Day*	15	30	30	35	55	30	3	22
		Intermediate Day	65	50	40	75	75	12	15	30
		Overcast Day	70	15	20	10	90	10	25	15
	GENSKY	*Clear Day*	70	30	25	35	85	55	5	25
		Intermediate Day	95	85	82	75	90	90	90	70
		Overcast Day	80	5	5	0	95	62	50	60
	GENDALYIT	*Clear Day*	60	30	22	35	85	45	5	50
		Intermediate Day	80	70	82	60	95	80	95	90
		Overcast Day	100	100	100	100	100	100	100	100

Appendix H: Clear day

Figures below illustrate simulated and measured daylight illuminance for the multiple sky models, in indoor environment under clear sky condition (for both horizontal and vertical sensors).

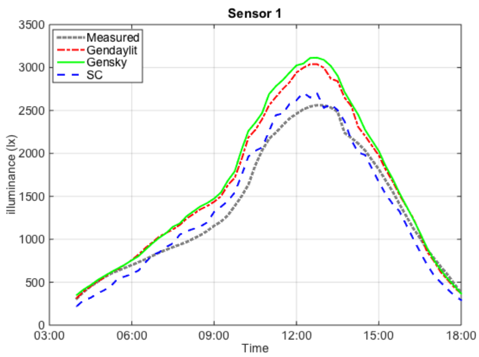

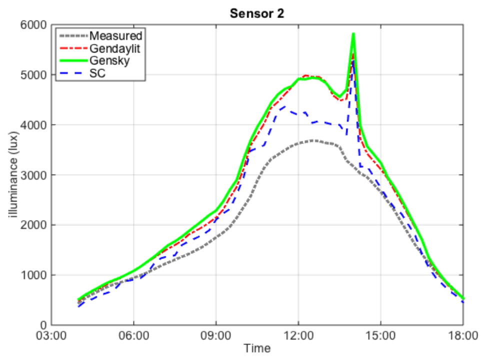

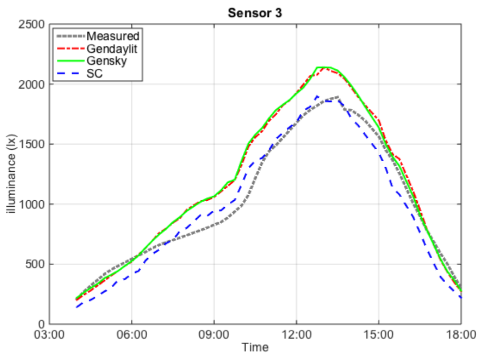

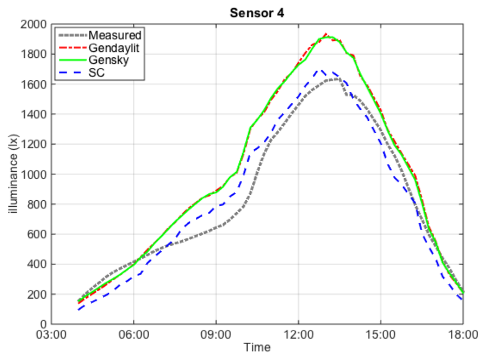

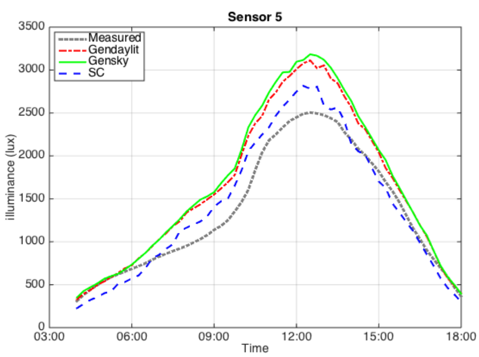

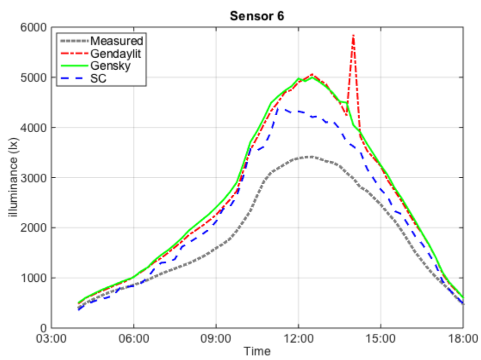

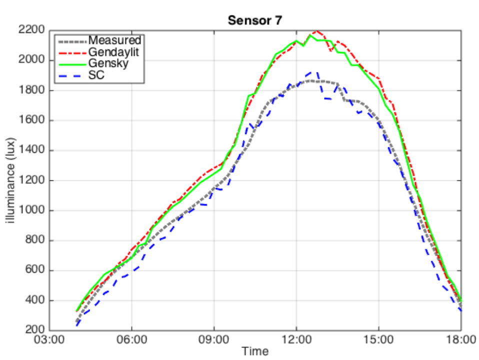

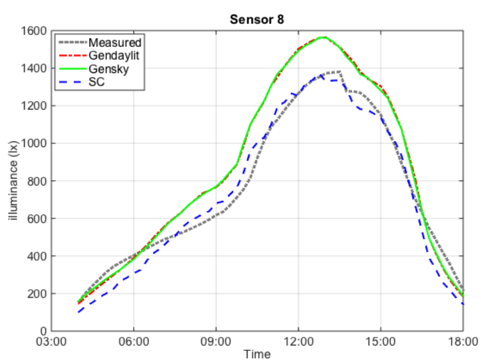

Figures below show the Cumulative Distribution Function (CDF) of the relative errors for the multiple sky models, in indoor environment under clear sky condition (for both horizontal and vertical sensors).

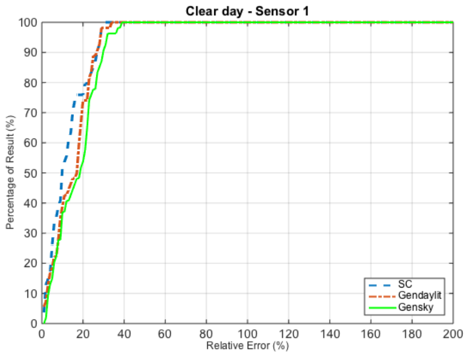

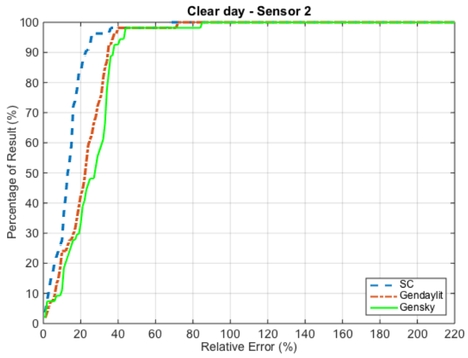

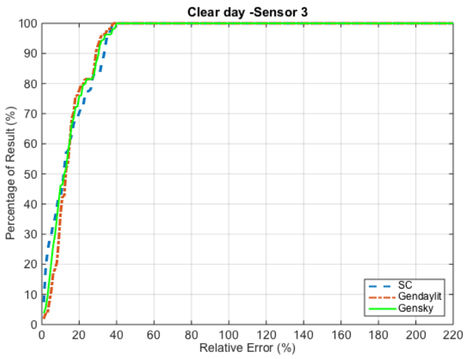

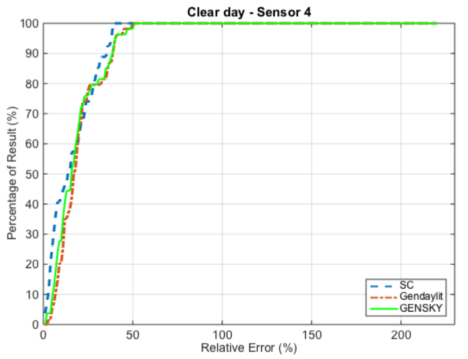

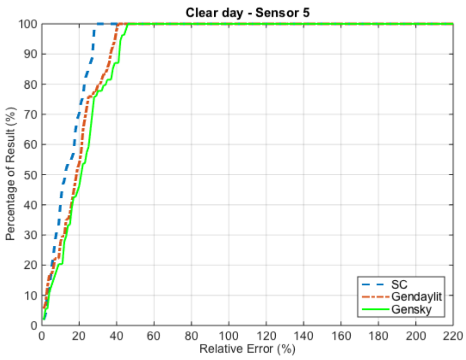

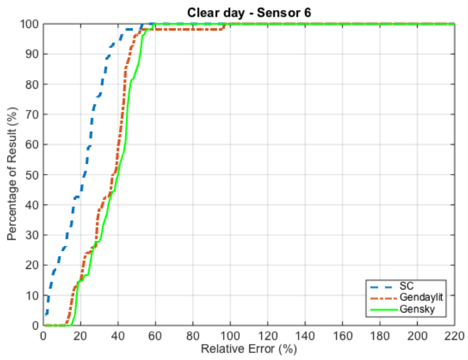

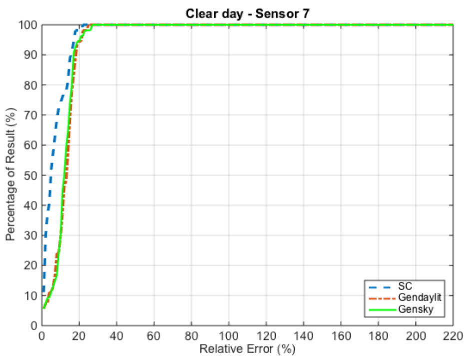

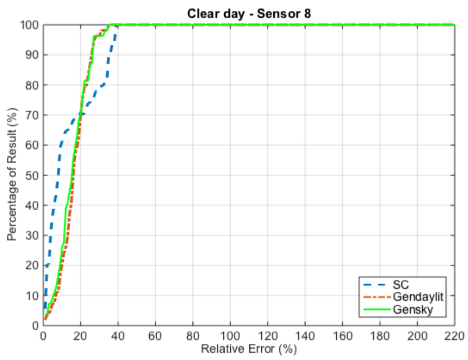

Appendix I: Overcast day

Figures below illustrate simulated and measured daylight illuminance for the multiple sky models, in indoor environment under overcast sky condition (for both horizontal and vertical sensors).

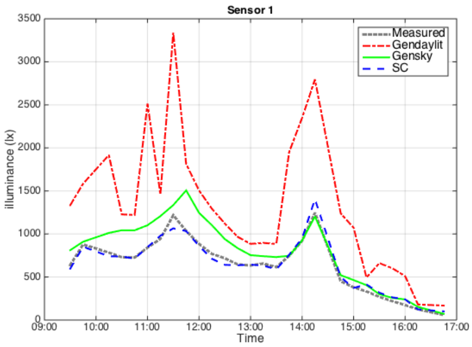

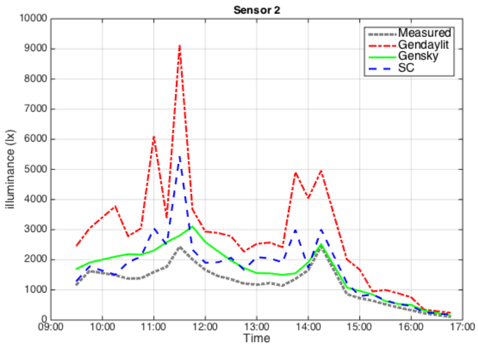

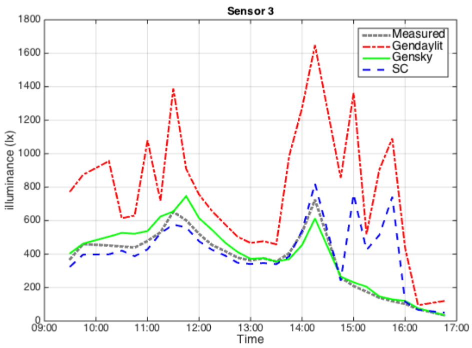

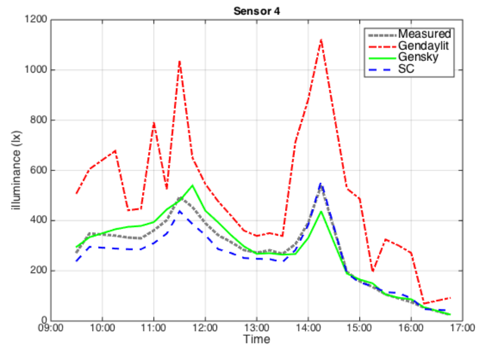

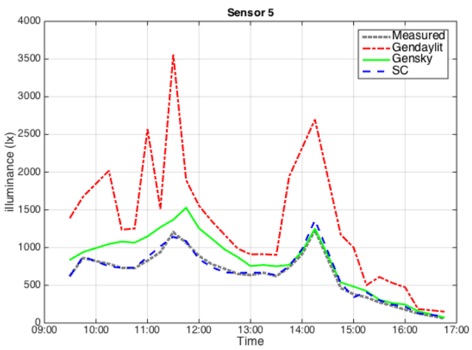

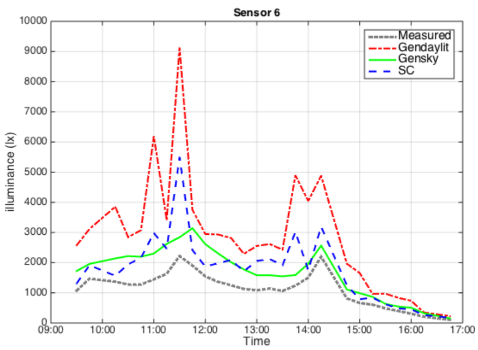

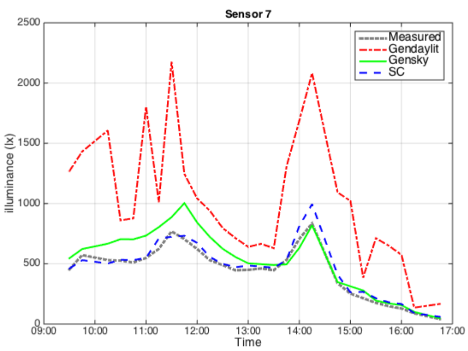

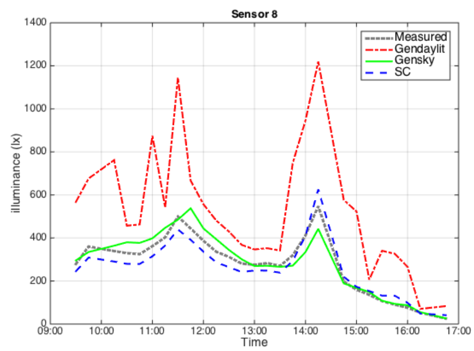

Figures below show the Cumulative Distribution Function (CDF) of the relative errors for the multiple sky models, in indoor environment under overcast sky condition (for both horizontal and vertical sensors).

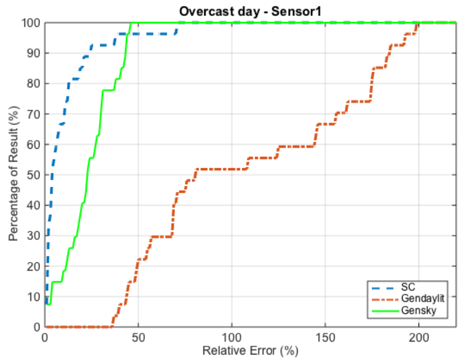

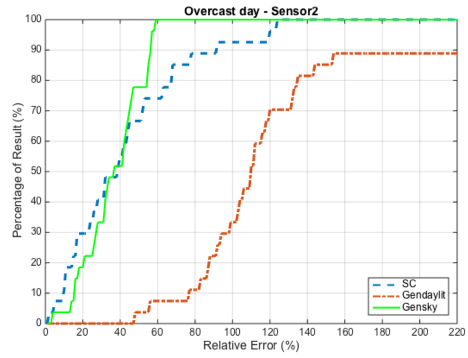

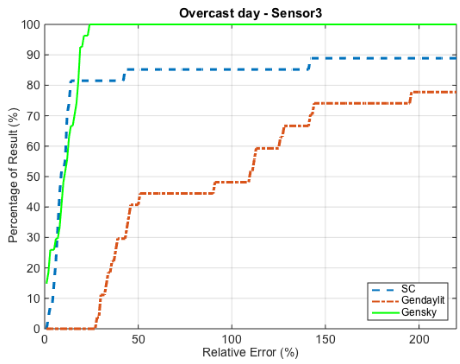

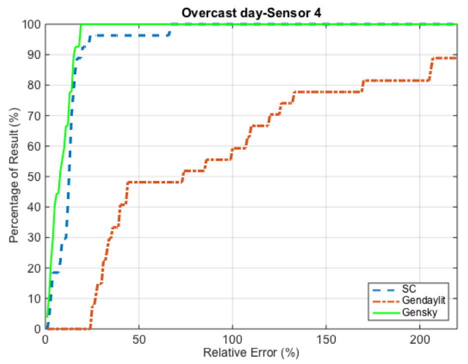

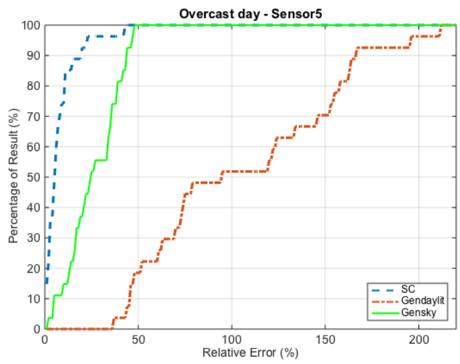

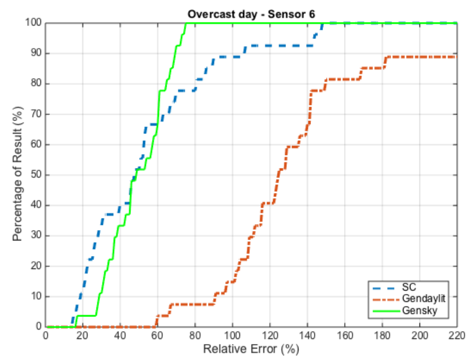

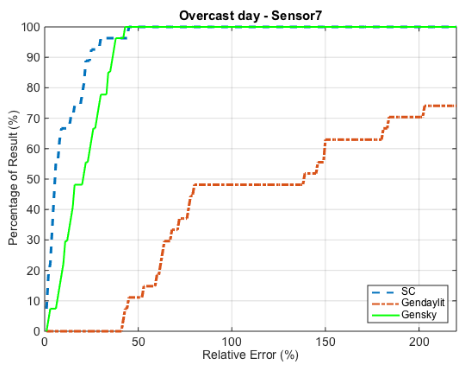

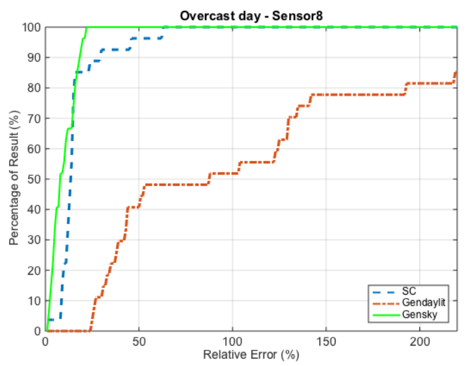

Appendix J: Intermediate day

Figures below illustrate simulated and measured daylight illuminance for the multiple sky models, in indoor environment under Intermediate sky condition (for both horizontal and vertical sensors).

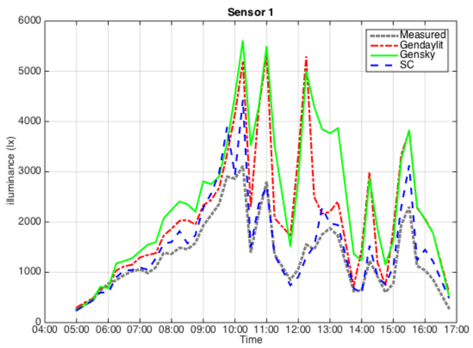

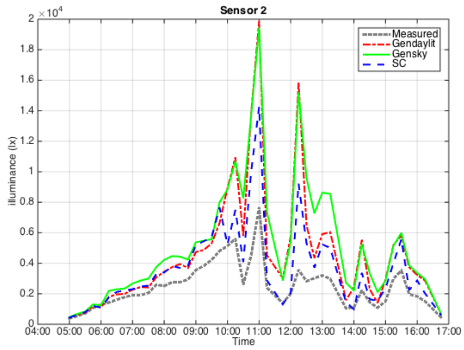

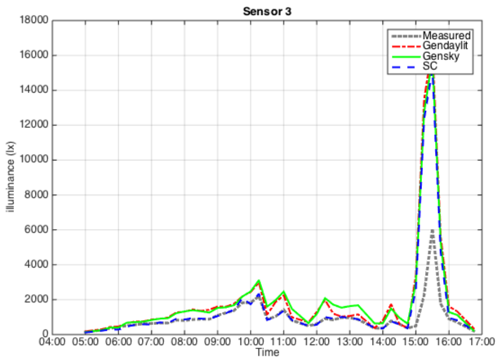

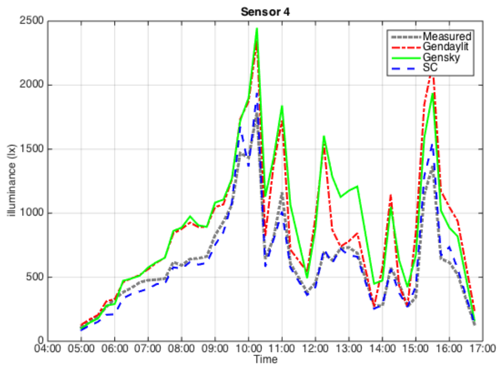

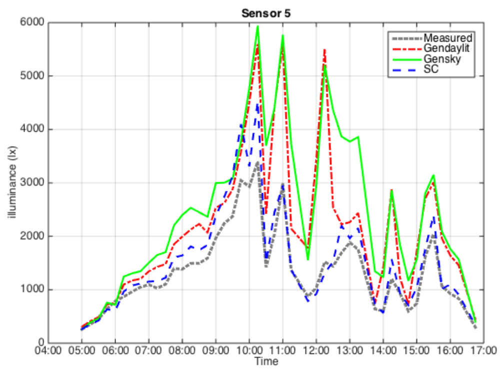

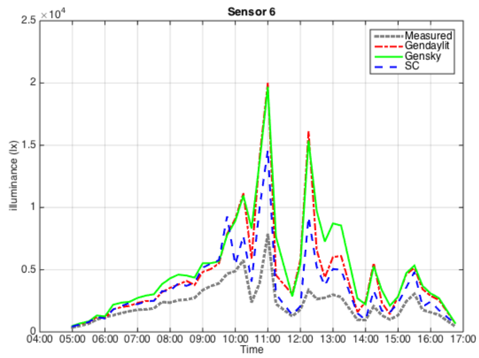

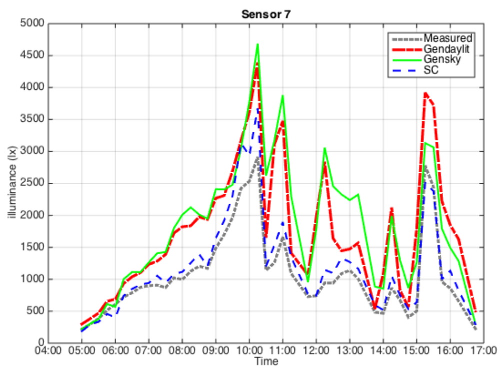

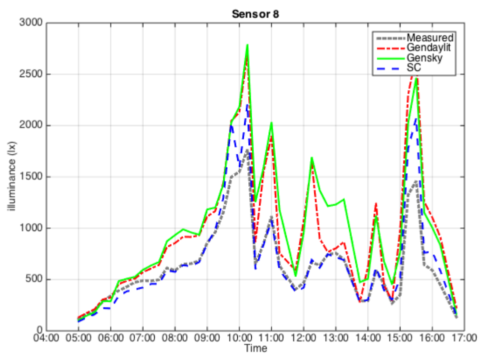

Figures below show the Cumulative Distribution Function (CDF) of the relative errors for the multiple sky models, in indoor environment under overcast sky condition (for both horizontal and vertical sensors).

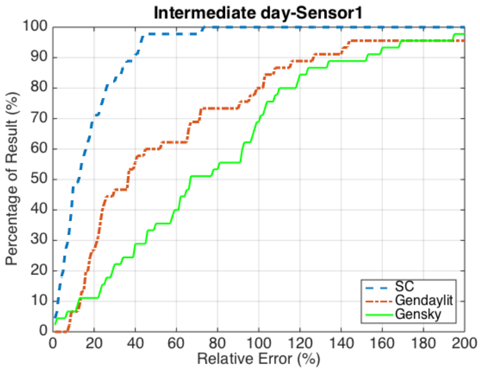

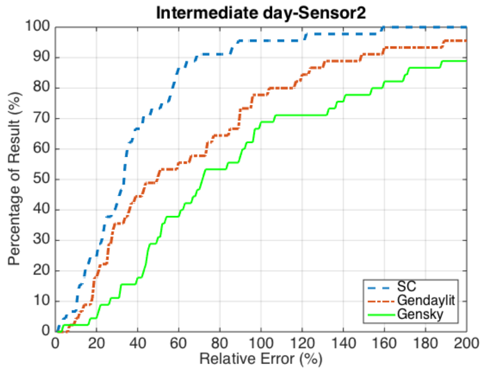

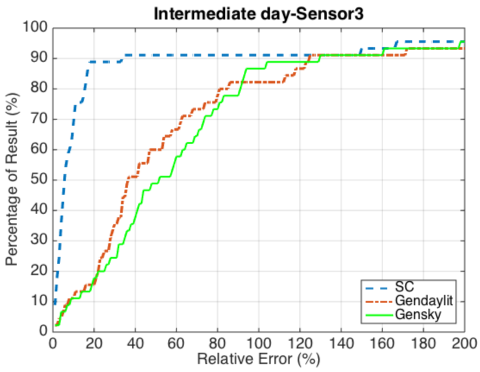

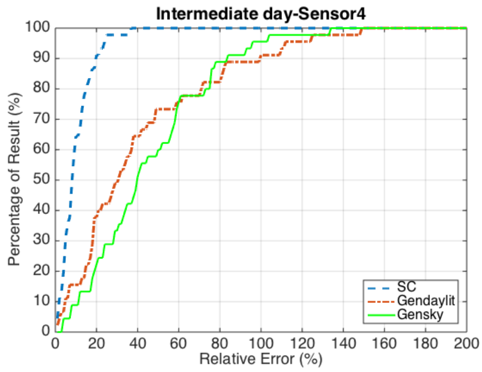

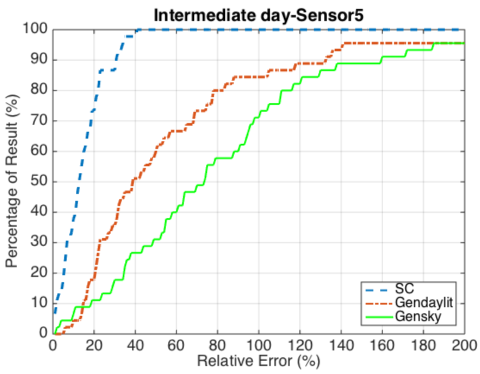

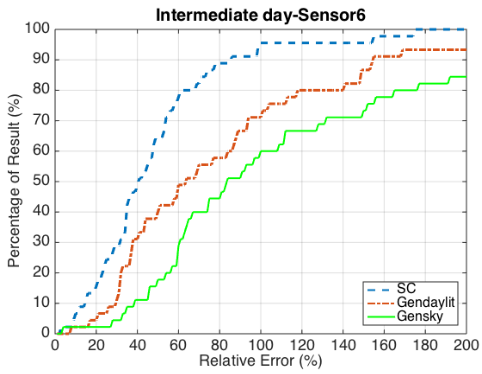

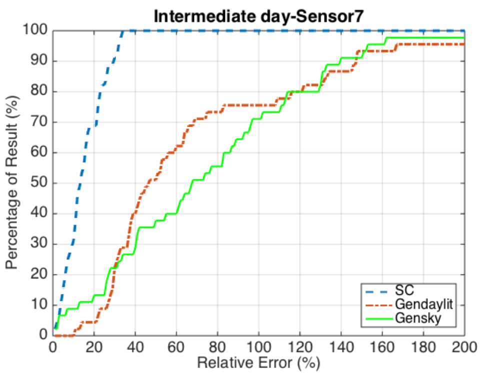

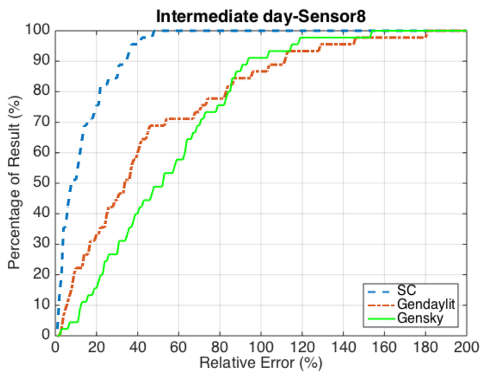

Appendix K: Error statistics for measured luminance efficacy

The default luminance efficacy in Radiance does not match the actual -measured - values. Assuming that accurate values of luminance efficacy would be available for a specific location, they could be applied. In our case, the use of the measured luminance efficacy (122 $W.m^{-1}$) would improve the performance of the Gensky and Gendaylit models. Tables below shows error statistics for horizontal (S1 to S6) and vertical (S7 and S8) indoor illuminance simulations under different sky conditions.

Clear Day	Sky model	MBE	RMSE	MAE	PR>20%RE
Horizontal	Gensky	-14	17	14	30
	Gendaylit	-16	18	16	40
Vertical	Gensky	-23	24	23	60
	Gendaylit	-23	24	23	60

Overcast Day	Sky model	MBE	RMSE	MAE	PR>20%RE
Horizontal	Gensky	-9	13	10	20
	Gendaylit	55	67	55	85
Vertical	Gensky	-21	23	21	50
	Gendaylit	61	69	62	50

Intermediate Day	Sky model	MBE	RMSE	MAE	PR>20%RE
Horizontal	Gensky	32	53	30	60
	Gendaylit	18	45	38	50
Vertical	Gensky	14	34	26	50
	Gendaylit	10	34	23	30